M.Sc. Physics

Neha Bhatt

2023

KALANCHOE FEDTSCHENKOI MEDIATED SYNTHESIS OF TUNABLE GOLD NANOPARTICLES FOR PROTEIN INTERACTION AND CATALYTIC ACTIVITY

A DISSERTATION

SUBMITTED IN PARTIAL FULFILLMENT OF THE REQUIREMENTS
FOR THE AWARD OF THE DEGREE
OF

MASTER OF SCIENCE

IN

PHYSICS

Submitted by:

Neha Bhatt

(2K21/MSCPHY/32)

Under the supervision of

DR. MOHAN SINGH MEHATA

DEPARTMENT OF APPLIED PHYSICS
DELHI TECHNOLOGICAL UNIVERSITY
(Formerly Delhi College of Engineering)
Bawana Road, Delhi – 110042

MAY, 2023

CANDIDATE'S DECLARATION

I, Neha Bhatt, Roll No. 2K21/MSCPHY/32, student of M.Sc. Physics, hereby declare that the project Dissertation titled "Kalanchoe Fedtschenkoi Mediated Synthesis of Tunable Gold Nanoparticles for Protein Interaction and Catalytic Activity", which is submitted by me to the Department of Applied Physics, Delhi Technological University, Delhi in partial fulfillment of the requirement for the award of the degree of Master of Science, is original and not copied from any source without proper citation. This work has not previously formed the basis for the award of any Degree, Diploma, Associate ship, Fellowship or other similar title or recognition.

- Paper published in Scopus indexed journal with following details:

  Title of Paper: "A Sustainable Approach to Develop Gold Nanoparticles with *Kalanchoe Fedtschenkoi* and Their Interaction with Protein and Dye: Sensing and Catalytic Probe"

  Authors Names (In sequence as per Research Paper): Neha Bhatt, Mohan Singh Mehata

  Name of the Journal: Plasmonics

  Status of Paper: Published

  Date of Communication: 04 February 2023

  Date of Acceptance: 28 February 2023

  Published Online: 09 March 2023

Place: Delhi

Date: 25 May 2023

Neha Bhatt

Dr. Mohan Singh Mehata
Former JSPS (Japan) and CAS (China) Fellow

Assistant Professor

Department of Applied Physics
Delhi Technological University
Bawana Road, Delhi – 110042
INDIA
Mob: +91 9953142553
Email: msmehata@dtu.ac.in
msmehata@gmail.com

SUPERVISOR CERTIFICATE

I, hereby certify that the Project Dissertation titled "Kalanchoe Fedtschenkoi Mediated Synthesis of Tunable Gold Nanoparticles for Protein Interaction and Catalytic Activity" which is submitted by Neha Bhatt, Roll No. 2K21/MSCPHY/32 to the Department of Applied Physics, Delhi Technological University, Delhi in partial fulfillment of the requirement for the award of the degree of Master of Science, is a record of the project work carried out by the student under my supervision. To the best of my knowledge, this work has not been submitted in part of full for any Degree or Diploma to this University or elsewhere.

Place: Delhi **DR. MOHAN SINGH MEHATA**

Date: 25 May 2023 **SUPERVISOR**

PROOF OF INDEXING

Plasmonics

Scopus Preview

Author Search Sources Create account Sign in

Source details

Feedback > Compare sources >

Plasmonics

Scopus coverage years: from 2006 to Present

Publisher: Springer Nature

ISSN: 1557-1955

Subject area: Biochemistry, Genetics and Molecular Biology: Biophysics | Biochemistry, Genetics and Molecular Biology: Biotechnology | Biochemistry, Genetics and Molecular Biology: Biochemistry

Source type: Journal

View all documents > | Set document alert | Save to source list | Source Homepage

CiteScore 2021
4.5

SJR 2021
0.484

SNIP 2021
0.671

Springer

Search | Authors & Editors | Log in

Plasmonics

Editorial board | Aims & scope | Journal updates

Plasmonics publishes peer-reviewed articles that both advance and report on the knowledge and practice of the interactions of free-metal electrons, Plasmons. Coverage includes theory, physics, and applications of surface plasmons in metals, and rapidly emerging areas of nanotechnology, biophotonics, sensing, biochemistry and medicine. The journal covers the theory, synthesis and optical properties of noble metal nanostructures, patterned surfaces, continuous or grated surfaces and devices. Applications include surface-enhanced spectroscopic properties, such as Raman scattering or fluorescence, as well developments in techniques such as surface plasmon resonance and near-field scanning optical microscopy. — show all

Editor
Chris D. Geddes

Publishing model
Hybrid (Transformative Journal). How to publish with us, including Open Access

2.726 (2021)
Impact factor

2.344 (2021)
Five year impact factor

63 days
Submission to first decision (Median)

202,063 (2021)
Downloads

You have access to our articles

For authors

Submission guidelines
Manuscript editing services
Ethics & disclosures
Open Access fees and funding
Contact the journal
Calls for papers

Submit manuscript

Working on a manuscript?
Avoid the most common mistakes and prepare your manuscript for journal editors.
Learn more →

PLAGIARSIM REPORT

WORD COUNT **9478 Words**	CHARACTER COUNT **53090 Characters**
PAGE COUNT **53 Pages**	FILE SIZE **8.9MB**
SUBMISSION DATE **May 17, 2023 7:32 PM GMT+5:30**	REPORT DATE **May 17, 2023 7:34 PM GMT+5:30**

9% Overall Similarity

The combined total of all matches, including overlapping sources, for each database.

- 6% Internet database
- 5% Publications database
- Crossref database
- Crossref Posted Content database
- 4% Submitted Works database

Excluded from Similarity Report

- Bibliographic material
- Small Matches (Less then 10 words)
- Manually excluded sources

9% Overall Similarity

Top sources found in the following databases:

- 6% Internet database
- 5% Publications database
- Crossref database
- Crossref Posted Content database
- 4% Submitted Works database

TOP SOURCES

The sources with the highest number of matches within the submission. Overlapping sources will not be displayed.

1	mdpi.com Internet	<1%
2	Mohan Singh Mehata. "Green route synthesis of silver nanoparticles us... Crossref	<1%
3	Universitas Pendidikan Indonesia on 2020-12-17 Submitted works	<1%
4	Smritimoy Pramanik, Paltu Banerjee, Arindam Sarkar, Subhash Chandr... Crossref	<1%
5	BRAC University on 2015-08-16 Submitted works	<1%
6	ntrs.nasa.gov Internet	<1%
7	nature.com Internet	<1%
8	eprints.uthm.edu.my Internet	<1%
9	ml.scribd.com Internet	<1%
10	Intercollege on 2017-09-14 Submitted works	<1%
11	espublisher.com Internet	<1%
12	José Gaete, Lorena Molina, Ian Alfaro, Joaquin Yañez, Fernando Valen... Crossref	<1%
13	Sreekanth, T.V.M., Min-Ji Jung, and In-Yong Eom. "Green synthesis of ... Crossref	<1%
14	researchsquare.com Internet	<1%
15	Sajjad Shamaila, Ahmed Khan Leghari Sajjad, Najam-ul-Athar Ryma, Si... Crossref	<1%
16	Yeungnam University on 2019-07-30 Submitted works	<1%
17	Asian Institute of Technology on 2009-07-25 Submitted works	<1%
18	Manoj B. Gawande, Anandarup Goswami, François-Xavier Felpin, Tewo... Crossref	<1%
19	discovery.ucl.ac.uk Internet	<1%
20	dspace.dtu.ac.in:8080 Internet	<1%

21	Babita Bisht, Pinki Dey, Avinash Kumar Singh, Sanjay Pant, Mohan Sing... Crossref	<1%
22	Swarup Roy, Jong-Whan Rhim. "Probing the binding interaction of lyso... Crossref	<1%
23	University of KwaZulu-Natal on 2015-12-10 Submitted works	<1%
24	coek.info Internet	<1%
25	issuu.com Internet	<1%
26	nanobioletters.com Internet	<1%
27	tudr.thapar.edu:8080 Internet	<1%
28	frontiersin.org Internet	<1%
29	hindawi.com Internet	<1%
30	Al Quds University on 2023-03-19 Submitted works	<1%
31	Maheshkumar Prakash Patil, Daniel Ngabire, Hai Ha Pham Thi, Min-Do ... Crossref	<1%
32	Nottingham Trent University on 2011-09-02 Submitted works	<1%
33	Ruby, Aryan, Mohan Singh Mehata. " Surface plasmon resonance allie... Crossref	<1%
34	Samiksha Shukla, Anne Masih, Aryan, Mohan Singh Mehata. "Catalytic... Crossref	<1%
35	The Robert Gordon University on 2016-01-21 Submitted works	<1%
36	core.ac.uk Internet	<1%
37	dx.doi.org Internet	<1%
38	etheses.bham.ac.uk Internet	<1%
39	rcastoragev2.blob.core.windows.net Internet	<1%
40	scielo.br Internet	<1%

Excluded from Similarity Report

- Bibliographic material
- Small Matches (Less then 10 words)
- Manually excluded sources

EXCLUDED SOURCES

link.springer.com Internet	76%
Neha Bhatt, Mohan Singh Mehata. "A Sustainable Approach to Develop Gold ... Crossref	74%
researchgate.net Internet	10%

Place: Delhi

Date: 25 May 2023

Neha Bhatt

Dr. Mohan Singh Mehata

Supervisor

ACKNOWLEDGEMENT

I would like to express my indebtedness and deepest sense of regard to my supervisor, Dr. Mohan Singh Mehata, Assistant Professor, Department of Applied Physics, Delhi Technological University for providing his incessant expertise, inspiration, encouragement, suggestions and this opportunity to work under his guidance. I am grateful for the constant help provided at every step of this project by Ms. Aneesha and all the lab members of Laser Spectroscopy Laboratory, Department of Applied Physics, Delhi Technological University. I am also thankful to my family and colleagues for their invaluable support, care and patience during this project. Lastly, I would thank Delhi Technological University for providing such a wonderful opportunity of working on this project.

ABSTRACT

In this study, highly stable gold nanoparticles (AuNPs) of different sizes ranging from 15-55 nm were synthesized via an eco-friendly, sustainable and cost-efficient approach using a new plant, *Kalanchoe Fedtschenkoi*. The AuNPs demonstrated an absorption spectrum at around 525 nm, hence exhibiting a strong surface plasmon resonance (SPR) band that is created when the free electrons of the AuNPs oscillate in harmony with the frequency of incident light. The impact of physiochemical environments, pH and temperature was examined. The crystal structure and stability of the produced AuNPs were validated with a X-Ray diffractogram, zeta potential analysis and absorption. The morphology, structure and bonds were examined using HRTEM and FTIR, respectively. The interaction of AuNPs (concentrations range of 0 - 181 μM) with plasma protein bovine serum albumin was explored using absorption and fluorescence studies. Further, AuNPs were utilized as an active catalyst for the degradation of dye methylene blue (MB) in the presence of $NaBH_4$. MB was degraded by 94 %, and the solution became colorless within 16 min with a rate constant of 0.175 min^{-1}.

CONTENTS

LIST OF FIGURES

LIST OF SYMBOLS AND ABBREVIATIONS

NPs	Nanoparticles
Au	Gold
AuNPs	Gold Nanoparticles
MB	Methylene Blue
KF	Kalanchoe Fedtschenkoi
HRTEM	High Resolution Transmission Electron Microscopy
NIR	Near Infrared
SPR	Surface Plasmon Resonance
BSA	Bovine Serum Albumin
DI	Deionized
XRD	X-Ray Diffraction
$HAuCl_4$	Chloroauric acid
UV-Vis	Ultraviolet – Visible
FTIR	Fourier Transform Infrared
FL	Fluorescence
FCC	Face Centered Cubic
JCPDS	Joint Committee on Powder Diffraction Standards
DLS	Dynamic Light Scattering
SH	Thiol
BH plot	Benesi Hildebrand Plot
Trp	Tryptophan
SV Plot	Stern-Volmer Plot
LoD	Limit of Detection

CHAPTER 1

INTRODUCTION

1.1. NANOTECHNOLOGY

Nanotechnology, a science that encompasses several disciplines and involves chemistry, physics, biology, environment, medicine and agriculture, has the potential to solve various problems such as drug delivery, solar energy conversions [1], wastewater treatment [2] and cancer treatment [3] and medicine. The ability of nanotechnology to control and modify the properties of materials at the atomic and molecular scale allows the creation of new materials and devices with enhanced properties and functionalities. In recent years, the astounding advancements in nanotechnology has attracted researchers to engage themselves in developing reliable and efficient methods to produce nanomaterials ranging from 1 to 100 nm [4]. Because of the variation from their bulk counterparts in terms of optical, electronic, physiochemical and magnetic properties, the interest in nanomaterials has intensified [5].

Major categories of nanostructures of biological significance include metallic, magnetic nanoparticles, semiconductor quantum dots, carbon-based, polymeric nanostructures. Quantum dot's size-dependent emission characteristics make them effective for biological identification and detection. For employment in cell sorting, magnetic nanoparticles have been used [6]. The interdisciplinary approach has enabled the creation of innovative solutions to complex problems, leading to new discoveries and advancements.

1.2. CRITICAL ANALYSIS OF EXISTING LITERATURE

1.2.1. Synthesis Routes

Numerous chemical and physical techniques have been employed for the large-scale synthesis of various nanomaterials [7]. Chemical approaches, including electrochemical technique [8], precipitation [9], sonochemical route [10], sol-gel, hydrothermal [11], chemical bath deposition [12], chemical reduction [13], chemical vapor deposition [14], microemulsion technique and microwave-assisted [15] synthesis are the main techniques through the chemical approach using harsh reducing agents, organic compounds and hazardous substances as well as producing hazardous by-products that are extremely damaging to the environment [16]. The physical methods of synthesis, such as gamma radiation, pulsed laser, plasma, vacuum vapor deposition [17] and mechanical milling, are quite time-consuming and require high energy. Given the limitations of chemical and physical processes, the growing concerns over environmental sustainability and the potential hazards associated with these methods, designing an efficient and ecologically friendly approach to producing nanomaterials is essential [18].

1.2.2. Gold Nanoparticles

Gold nanostructures and the 0-D nanoparticles (AuNPs) are one of the most commonly used noble metal nanoparticles (NPs) and are applied in a variety of fields [19]. Some of the important physical properties of gold are represented in Fig. 1.1. AuNPs exhibit size and shape dependent catalytic, optical, and electrical properties, making them useful for a variety of applications. AuNPs have proven to be an efficient choice for a variety of purposes such as leukemia therapy [20], biomolecular immobilization [21],

biosensor production [22], cancer therapy [23], antibacterial treatments [24], antimicrobial treatments [25] and labeling for contrast enhancement in cryoelectron microscopy [26]. Apart from biological applications, AuNPs have been utilized in various other applications, including catalysis, detection [27] and optoelectronic devices [28]. The surface plasmon resonance (SPR) observed in AuNPs, which depends on suspension medium and particle morphology, is responsible for a wide range of applications of AuNPs [29].

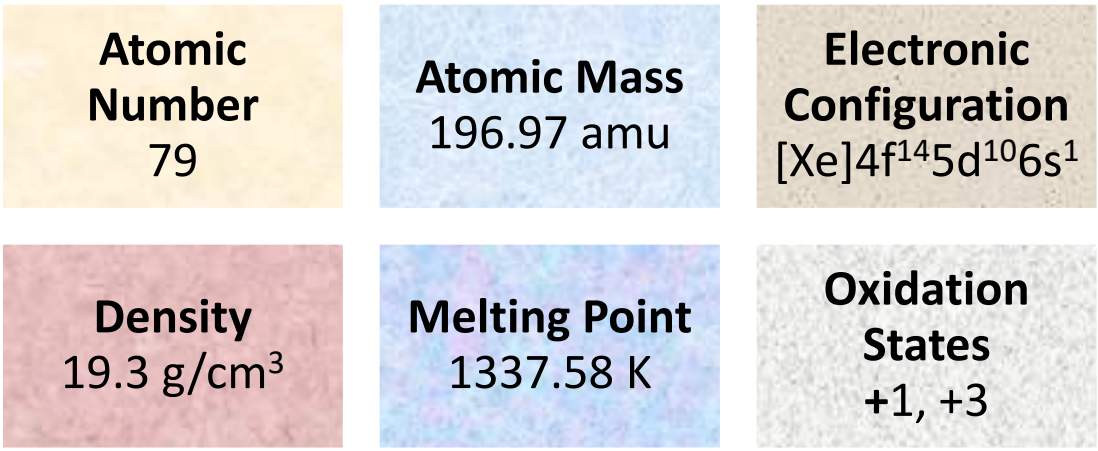

Figure 1.1. Physical Properties of Gold

1.2.3. Eco-Friendly Synthesis of Gold Nanoparticles

AuNPs have been prepared using several techniques, such as chemical, physical and biological methods. The most effective and environmentally benign approaches are biological ones, which draw on natural resources like plant components, agricultural wastes, enzymes, moulds, yeasts, bacteria, fungus and algae [15]. The need for environmentally friendly nanoparticle production developed because physical and chemical procedures are expensive and environmentally harmful. Additionally, the high cost and complexity of these methods can limit their widespread application. Green synthesis of nanoparticles utilizes environment-friendly, non-toxic, and secure

natural agents [30]. Since they are produced using a one-step process, nanoparticles created utilizing green technologies have a variety of optimum sizes, remarkable stability, and various natures [31]. The issue of toxic surface compounds is not present in nanoparticle synthesis using biological techniques [16]. AuNPs were synthesized from various sources, for example, using *Zingiber officinale* extract [32], *Honey* extract [33], *Murraya Koenigii* leaf [34], *Rosa hybrida* petal [35], *Trachyspermum ammi* seeds [5], *Macrotyloma uniflorum* [36], *Adiantum philippense L. Frond* [37], *Punica granatum* [38], *Salvia officinalis*, *Lippia citriodora*, *Pelargonium graveolens* [39], *Annona Squamosa L.* peel [15], *Dendropanax morbifera* leaf [40], *Allium ampeloprasum* leaf extract [41], *Nyctanthes arbortristis* flower [42], *Morinda citrifolia* leaf [43], *Trigonella foenum-graecum* [44], *Couroupita guianensis* flower [3], etc.

1.3. *KALANCHOE FEDTSCHENKOI*: A Green Ally in AuNPs Synthesis

The *Kalanchoe* plant, commonly known as “Lavender Scallops” or “South American air plant” is a perennial succulent plant which belongs to the *Crassulaceae* and is mostly found in Madagascar and Southeast Africa, is distributed worldwide in warm regions [45]. In these tropics, plants of the genus *Kalanchoe* are utilized as traditional remedies and have a variety of other ethnobotanical purposes. This species is employed as an analgesic in Brazil. In traditional medicine, the plant had been used to treat various ailments, including wounds, burns, rheumatism, and hypertension. The antibacterial properties of the plant were demonstrated by the growth inhibition exhibited by *K. fedtschenkoi* (KF) extracts displayed opposing gram-negative bacteria

species such as *P. aeruginosa* and *A. Baumannii*,, along with the gram-positive bacteria *S. aureus* [46].

1.4. BOVINE SERUM ALBUMIN (BSA)

Bovine serum albumin (BSA) is crucial for maintaining the blood pH and osmotic pressure as well as for transporting, binding, and delivering numerous substances to their intended organs [47]. Since the structure and characteristics of BSA are well understood, it is utilized as a model for research of conformational changes following interaction with AuNPs [48]. The structure of BSA involves 583 amino acid residues forming a single polypeptide chain, 17 disulfide links with a single thiol (SH) group. The BSA molecule is quite compact due to the presence of these disulfide bonds, which also help stabilize the helical structure of BSA. Fatty acids, which are insoluble in plasma, are transported mainly by BSA. The adsorption of serum albumins to metal oxides and the interaction of BSA with metal hydroxide suspensions have been thoroughly investigated [48]. However, it is known that the chemistry of the particle's surface and the protein's conformational state both significantly impact how proteins interact with AuNPs [49]. This makes it challenging to study the behavioral conformity of proteins for a nanoparticle-protein system, as protein adsorption can lead to the denaturation of the protein's tertiary and secondary structures [50].

Absorption and fluorescence spectroscopy are the most critical techniques for examining the interactions between metals and proteins due to their high sensitivity and straightforwardness [51]. Tryptophan residues Trp 134 and Trp 213 have the greatest impact on BSA's fluorescence (FL) [52]. Tyrosine and phenylalanine (Phe) residues make up only a tiny percentage of the yield due to their low FL quantum yield.

As reported previously, the alterations in the area around the microenvironment of residues may account for the variations of protein conformation on adding 2-azido acrylates [53]. The absorption or optical density maxima of BSA is located at 278 nm, with the fluorescence maxima of BSA appearing at 351 nm, quenched by adding AuNPs [54]. A putative conjugation mechanism is also proposed after looking at the conformational changes in BSA when interacting with AuNPs, based on the evidence gained using these approaches.

1.5. DEGRADATION OF HARMFUL DYES

One of the main issues with environmental degradation is the water contamination brought on by industrial development. Harmful dyes are widely used in industries such as food, textile, cosmetics, plastics, printing and packaging, leather, paper, and their discharge into the environment can cause significant ecological and health problems. Water contamination is influenced by a number of variables, one of which is the presence of synthetic dye in wastewater [55]. The release of water waste containing many organic dyes might obstruct plant photosynthesis and sunlight absorption. In addition, a lot of synthetic dyes pose a serious threat to human health [56]. These challenges have been overcome using various techniques, including chemical oxidation, adsorption, fabric filtration, and catalytic degradation [57].

Owing to their novel physical, chemical, and electrical characteristics, differing from their bulk counterparts, catalytic degradation using metal nanoparticles offers a convenient degrading approach for hazardous dyes among these techniques [58]. Using biocompatible, environmentally safe nanocatalyst to degrade toxic dyes is the simplest approach that does not require using organic solvents [59]. The aromatic dye

methylene blue (MB) has a heterocyclic structure. The colour of MB in its crystallized state is greenish-brown. MB solutions in water are blue. MB is a harmful industrial dye and is employed as a staining agent in the field of medicine [60].

1.6. AIM AND SCOPE OF STUDY

i. Green source mediated synthesis of stabilized gold nanoparticles at various physiological parameters.

ii. Analyzing the crystal structure, morphology and stability of the biosynthesized AuNPs using characterization techniques.

iii. Investigating the interaction of AuNPs with BSA protein for enhanced stability and protein properties.

iv. Exploring the catalytic behavior of AuNPs in degradation of toxic dye.

CHAPTER 2

EXPERIMENTAL SECTION

2.1. CHEMICALS

$HAuCl_4.H_2O$ (Tetrachloroauric (III) acid), Sodium borohydride ($NaBH_4$) and Sodium hydroxide (NaOH) were procured from Sigma-Aldrich Chemicals Co. Bovine albumin fraction V (BSA) and methylene blue dye were procured from CDH Chemicals Ltd. The chemicals were all utilized in their original form without any modifications. Deionized water (DI), having a specific resistance of 18.2 MΩ cm^{-1}, was employed as a solvent for all experiments.

2.2. PROTEIN SOLUTION

1.67 mg of BSA was added to 50 mL DI water to prepare a 0.5 µM solution. This solution was stirred for about 15 minutes to mix well and reached an equilibrium state. The solution was used for investigating the connection between BSA and AuNPs through absorption and fluorescence analysis.

2.3. DYE SAMPLES

Initially, a stock solution of 50 µM of MB dye (formula: $C_{16}H_{18}N_3SCl$; M.M.: 319.85 g/mol) was prepared by mixing 200 mL of DI water and 3.2 mg of the dye. This was further diluted to 10 µM by adding 80 mL of DI water to 20 mL of the stock solution. This solution was divided into three vials with 20 mL each. The first solution was degraded by $NaBH_4$, the second by AuNPs and the third by $NaBH_4$ + AuNPs. The amount of AuNPs added, 2 mL, was kept the same for both the second and third vials.

2.4. PREPARATION OF PLANT EXTRACT

Fresh *Kalanchoe Fedtschenkoi* (KF) leaves were picked from Dehradun, Uttarakhand, India, for use in this study. The leaves were further cleansed two to three times to remove impurities present on the surface. These leaves were dried in the oven at 75 °C for about a day until all the surface moisture was obliterated. The leaves were further crushed to form a fine powder. 2g powder was boiled with 50 mL of DI water for 30 min at 75 °C, which was further filtered using Whatmann filter paper and kept at a temperature of 4 °C in the refrigerator for further use. Figure 2.1 illustrates a schematic representation of the preparation of plant extract.

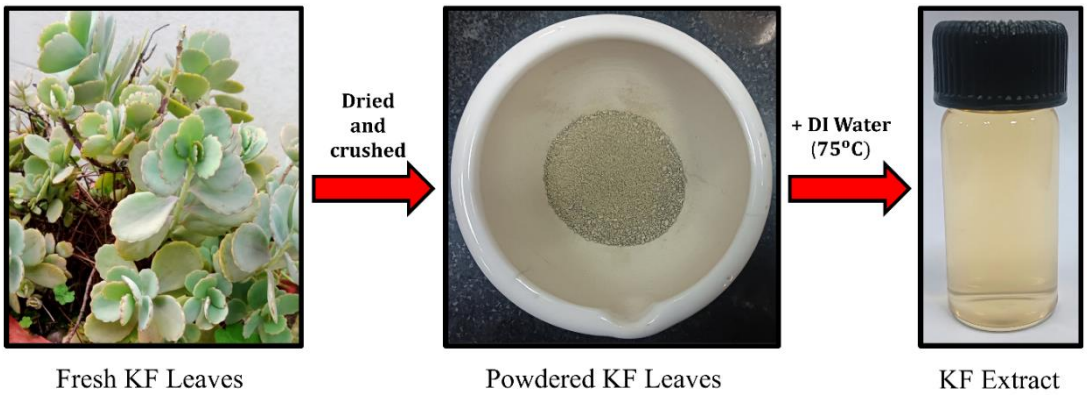

Figure 2.1. The schematic diagram for the preparation of plant extract

2.5. GOLD NANOPARTICLES SYNTHESIS

33.98 mg of $HAuCl_4$ was added to 100 mL of DI water to prepare 1 mM of tetrachloroauric acid solution. 40 mg of NaOH was stirred in 10 mL DI water for the preparation of 0.1 M solution of NaOH. 10 mL of 1mM chloroauric acid solution was placed in a conical flask and subjected to heating at 75 °C at 400 rpm for a duration of 15 minutes. Further, 2 mL of *Kalanchoe Fedtschenkoi* extract was added to the solution. The heating was turned off. A few drops of the basic solution of NaOH were

introduced into the mixture to adjust the pH to ~ 7 and decrease the reaction time. The mixture changed from light yellow to various shades from colorless, purple, light pink, pink and finally red as the reaction progressed over time. Various samples were formed, namely S1, S2, S3, S4 and S5, corresponding to their reaction time of 1, 2, 4, 6 and 8 h, respectively, to gain a deeper understanding of the formation mechanism and to control the size of the AuNPs. The longer and continuous reduction of gold nanoparticles leads to the formation of more uniform and symmetrical nanoparticles [61]. These samples were stored in the refrigerator for further examination. The illustration of the process of synthesizing gold nanoparticles is depicted in Figure 2.2, along with the color change.

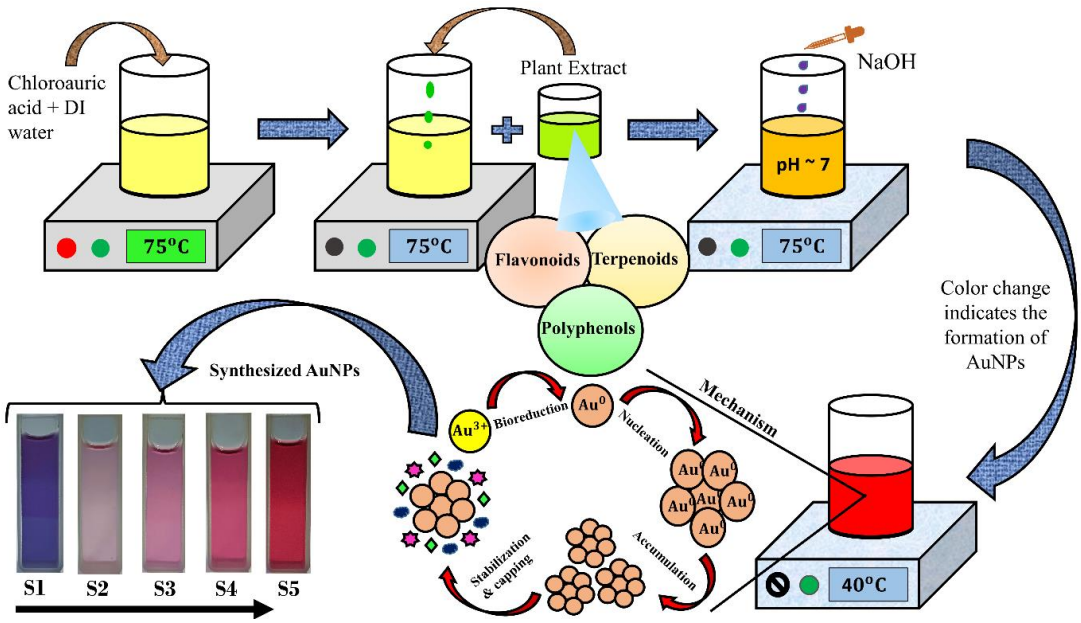

Figure 2.2. Synthesis of gold nanoparticles using the eco-friendly and cost-effective route

CHAPTER 3

CHARACTERIZATION TECHNIQUES

UV-visible absorption and fluorescence spectroscopy are the most frequently employed methods to identify active species due to their robust functionality and high sensitivity, even to small samples. Perkin-Elmer, Lambda 750 UV/VIS/NIR dual beam spectrometer (Fig. 3.1) was utilized for the UV-Vis spectroscopic studies. A Horiba Jobin Yvon Fluorolog-3 spectrofluorometer (Fig. 3.2), equipped with xenon and flash lamps with 450 W power and a photomultiplier tube, was used for steady-state FL and FL-excitation measurements. A quartz cuvette was used as a sample container having an optical path of 10 mm. Drop-casting was used to coat the colloidal AuNPs on a glass substrate in order to prepare a thin film of AuNPs to measure the X-ray diffractogram. BRUKER-D8 advanced (Fig. 3.3) was used to record the XRD pattern of a thin film of AuNPs.

Figure 3.1. PerkinElmber Lambda 750 UV/Vis/NIR spectrophotometer

Figure 3.2. Horiba Jobin Yvon Fluorolog-3 spectrofluorometer

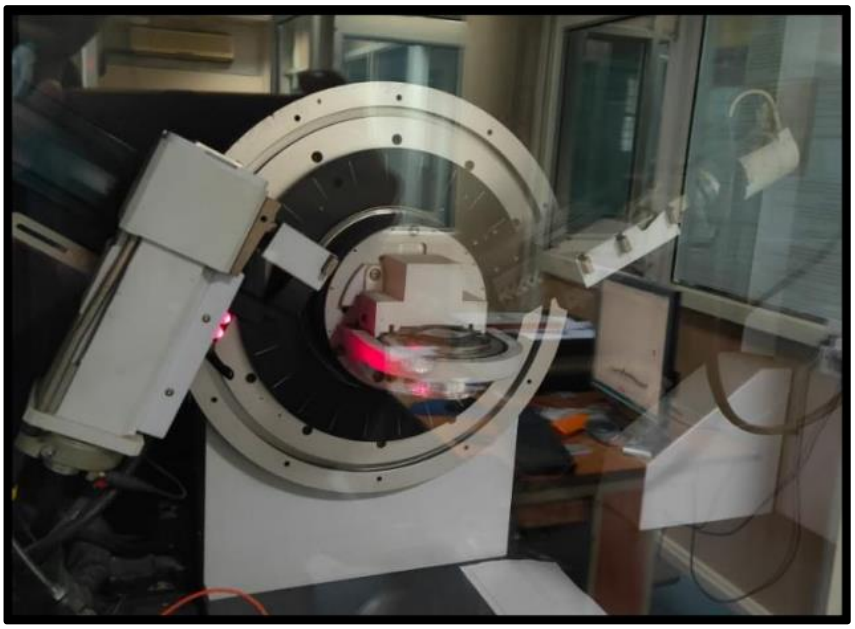

Figure 3.3. Bruker's D-8 Advanced X-Ray Diffractometer

TALOS thermo-scientific instrument (Acc. Vol. 200 kV) (Fig. 3.4) was used to record the high-resolution transmission electron microscopic (HR-TEM) images. The zeta potential of colloidal AuNPs along with the size distribution were recorded using a Zetasizer nano series ZS (Malvern Panalytical) (Fig. 3.5). Fourier transform infrared

(FTIR) studies in 400 to 4000 cm^{-1} were carried out using Perkin Elmer Two–Spectrum FTIR spectrometers (Fig 3.6). Furthermore, BSA was used in experiments with increasing concentrations of AuNPs ranging from 0.91 µM to 181 µM.

Figure 3.4. TALOS thermo-scientific instrument (Acc. Vol. 200 kV)

Figure 3.5. Zetasizer nano series ZS (Malvern Panalytical)

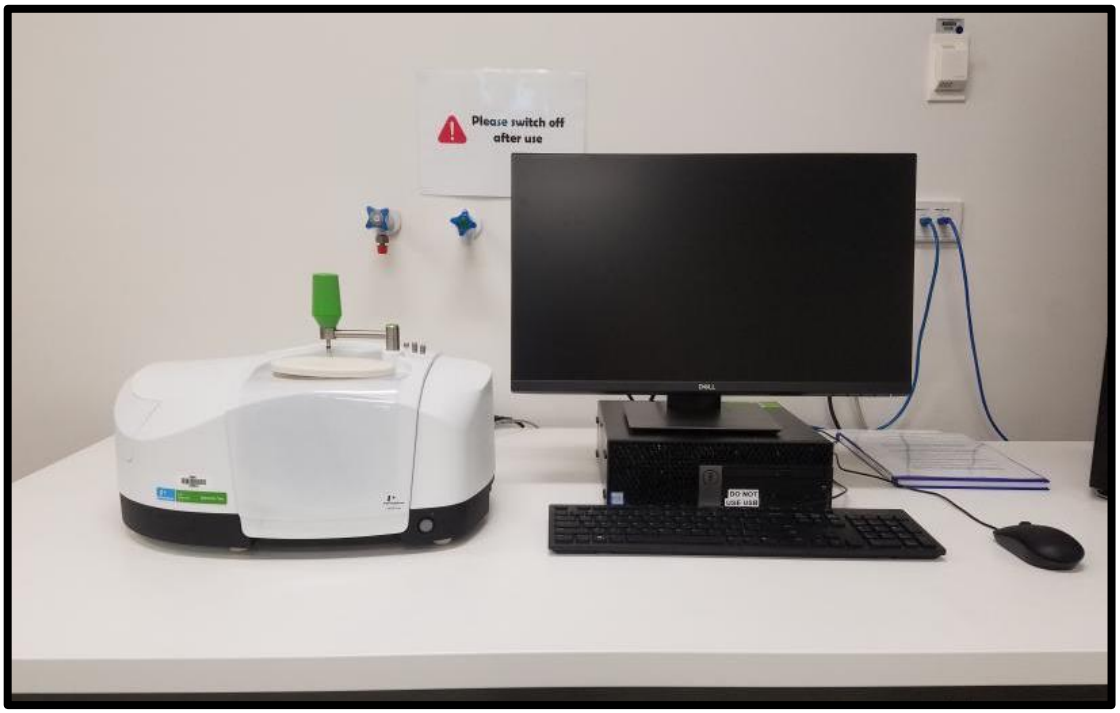

Figure 3.6. Perkin Elmer Two–Spectrum FTIR spectrometers

CHAPTER 4

RESULTS AND DISCUSSION

4.1. X-RAY DIFFRACTION ANALYSIS

The XRD pattern for biosynthesized AuNPs of sample S5 (a thin film of AuNPs overlay on a glass substrate) along with the JCPDS data of AuNPs is represented in Fig.4.1. The XRD peaks occur at 2 θ = 77.80°, 64.88°, 44.64° and 38.40°, and were indexed as (311), (220), (200) and (111) planes, respectively, based on the FCC structure of AuNPs (JCPDS. file no. 04-0784) [62]. The acquired XRD pattern showed that the synthesized AuNPs were crystallite in nature, which was confirmed by comparing it to the standard pattern for AuNPs. The intense diffraction peak at 38.40° indicates the favored direction of orientation in (111) direction [63]. This describes that molecular-sized structures have an identical spacing between each atom or molecule in a repeating 3D pattern [64]. The average crystallite size estimated using Debye-Scherer's equation D = 0.9 λ / β cos θ was 18 nm.

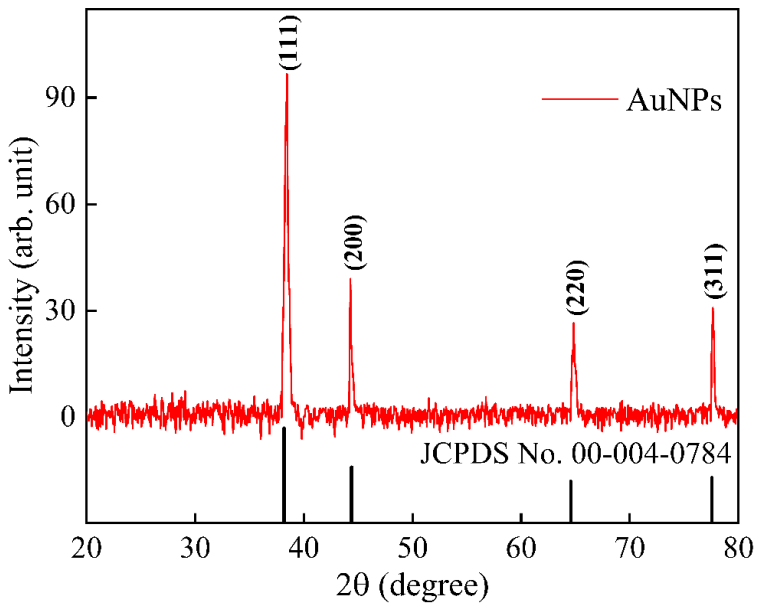

Figure 4.1. XRD pattern of synthesized AuNPs film

4.2. UV-VIS ABSORPTION SPECTRA

The size, shape, refractive index and interaction of gold colloids with their medium affect the surface plasmon resonance band of AuNPs that is appearing in the UV-Vis spectrum [44]. It is observed that the maximum plasmon resonance peak of gold nanoparticles varies from 561 to 525 nm with varying average particle sizes from S1–S5. Fig. 4.2(a) shows the absorption spectra of KF extract, $HAuCl_4$ solution and gold nanoparticles (S5). Fig.4.2(b) shows normalized absorption spectra of five different-sized AuNPs. The SPR band of colloid S1 occurs at 561 nm. This long wavelength absorption is caused by the SPR occurring within the plane, which indicates a notable difference in the shape of the AuNPs [65]. The size of the nanoparticles may be correlated linearly with the absorption wavelength [51]. From the spectra, it can be observed that as the reaction time increased from 1 to 8 h, the SPR band was seen to shift towards the shorter wavelength, indicating a decrease in particle size. Therefore, it can be mentioned that the reaction time plays an important role in influencing the shape and size distribution of AuNPs.

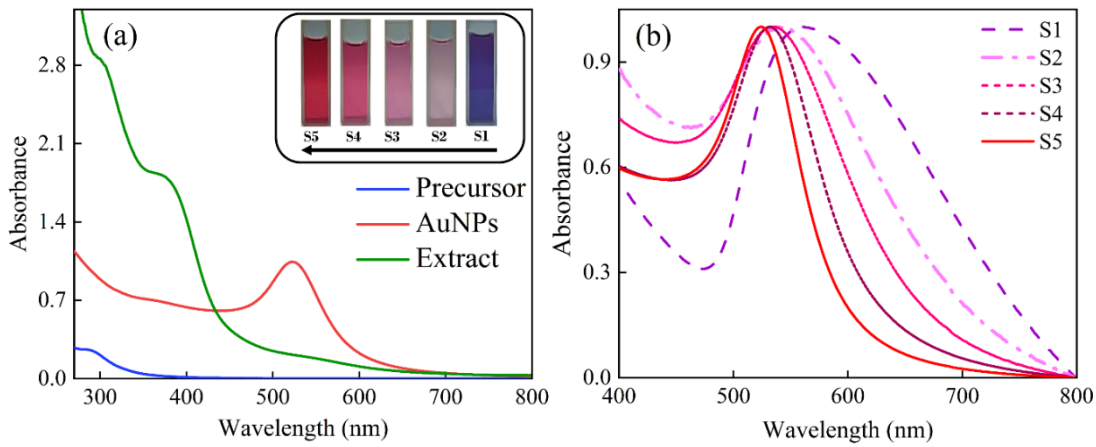

Figure 4.2. Absorption spectra (a) of precursor, plant extract and AuNPs (S5) along with color change (insets) and (b) normalized absorption spectra of different-sized AuNPs (S1=52 nm and S5=19 nm)

4.2.1. Effect of pH

The size and shape of AuNPs are greatly controlled by the pH of the solution. The absorption spectra of colloidal AuNPs produced at different pH levels between pH level 5 and 13 are displayed in Fig.4.3. Increasing the pH from acidic towards neutral (~5 - 8) increases the absorption intensity and reaches a maximum at pH 8. However, a further increase in pH beyond 8, from 8-13, results in a drop in absorption intensity. The electrical charges on biomolecules are altered by changes in pH, which also affects the peculiarities of the capping and stabilizing agents [61]. Although, the change in pH of the AuNPs colloidal solution did not bring any significant change in the position of the peak of the absorption band. Some aggregations are possible with further increasing of pH [56]. This indicates that pH 8 is optimal for synthesizing AuNPs with *Kalanchoe Fedtschenkoi* extract.

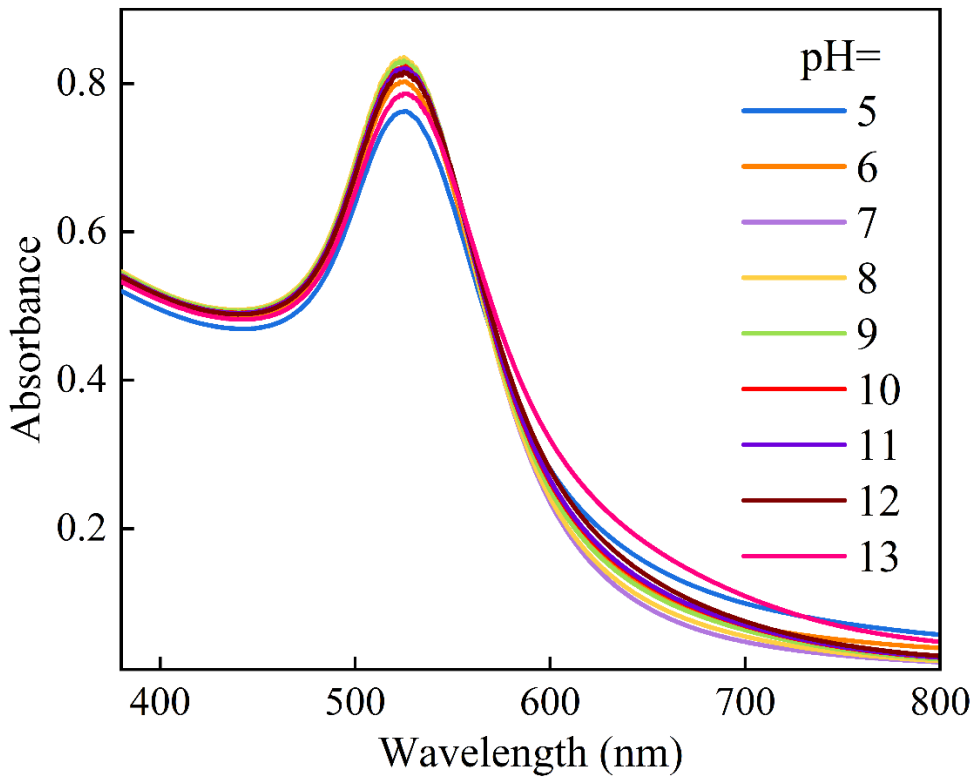

Figure 4.3. Absorption spectra of colloidal AuNPs at different pH

4.2.2. Effect of Temperature

The morphology of the synthesized AuNPs can be greatly impacted by the temperature [66]. Figure 4.4 shows the absorption spectra of the synthesized colloidal AuNPs (S5) at temperatures ranging from 0˚C to 100˚C at an interval of 10 ˚C. The absorption maximum and intensity of AuNPs show no significant variation for numerous temperatures. However, at 90˚C and 100˚C, there is a slight decrease in the absorbance intensity, that might be due to the effect of agglomeration of nanoparticles at high temperatures. The observed results indicate that the synthesized AuNPs are stable at various temperatures and agree with the previous report [67].

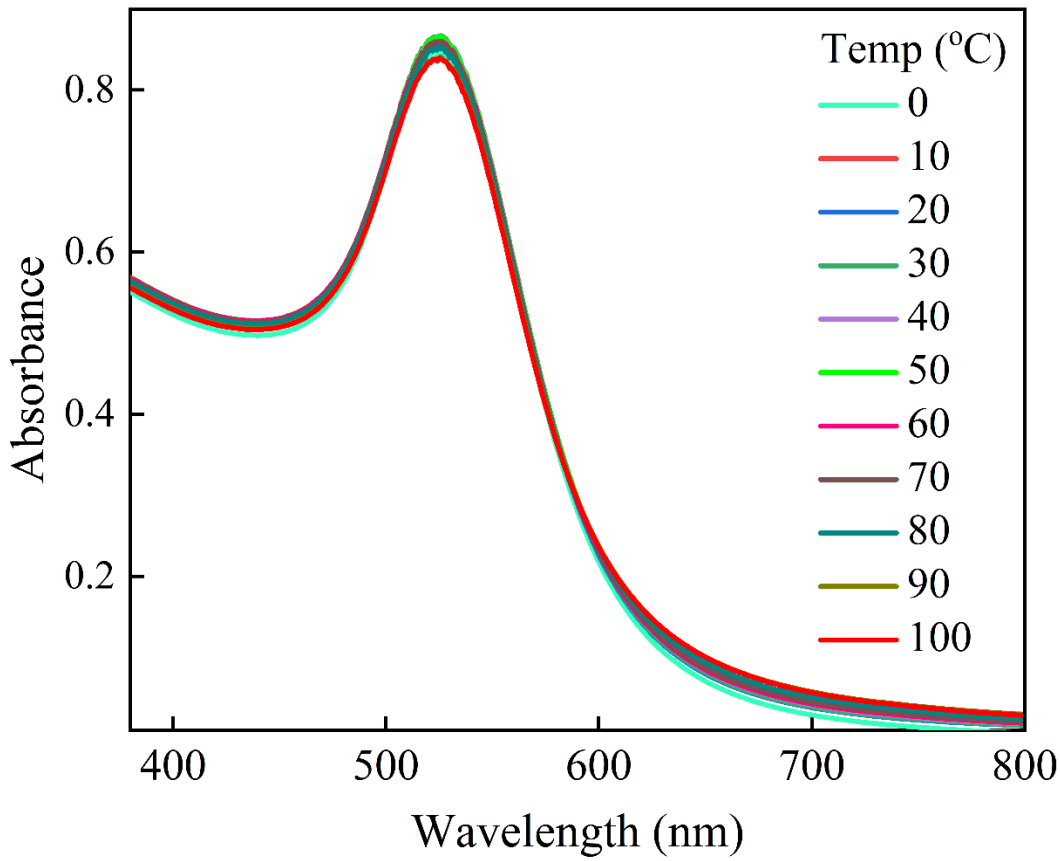

Figure 4.4. Absorption spectra of colloidal AuNPs at different temperatures

4.2.3. Stability of AuNPs

One of the critical parameters determining the stability of AuNPs is the period at which they hold without significant change in their properties. The more stable AuNPs can be utilized successfully for various biomedical applications. The absorption spectra of synthesized AuNPs (S5) were measured at an interval of 10 days for about 4 months. Figure 4.5 shows the absorption spectra for AuNPs recorded for 110 days at an interval of 10 days. A slight decrease in the absorption intensity was noticed even after 110 days without any shift in the maximum absorption wavelength. Therefore, the AuNPs synthesized using *Kalanchoe Fedtschenkoi* were far more stable than the stability observed in previous works [68], where the change in absorbance was quite significant in 10 days only. The change in absorption intensity for 110 days at interval of 10 days is represented in Fig. 4.6.

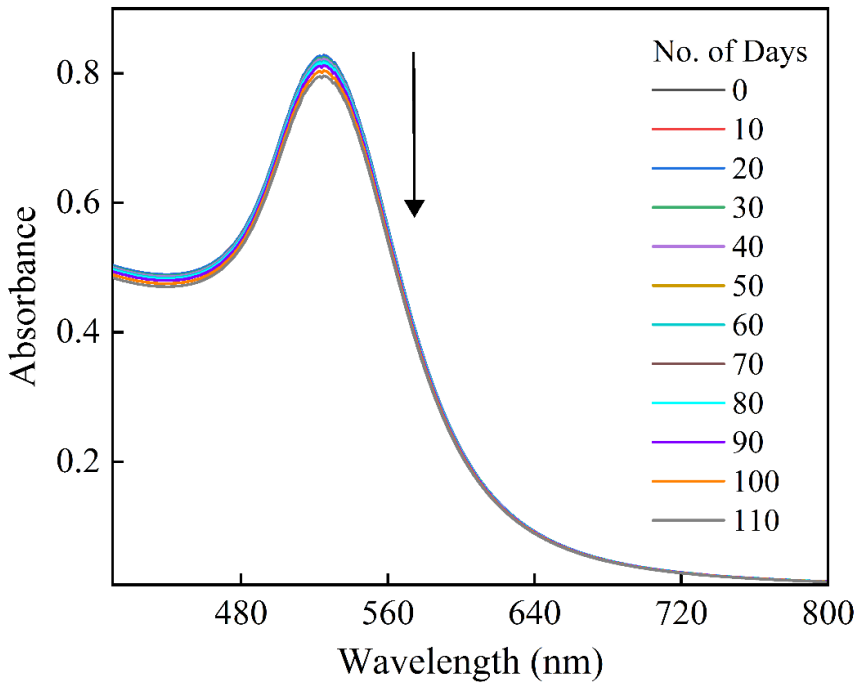

Figure 4.5. Absorption spectra of colloidal AuNPs on different days showing excellent stability

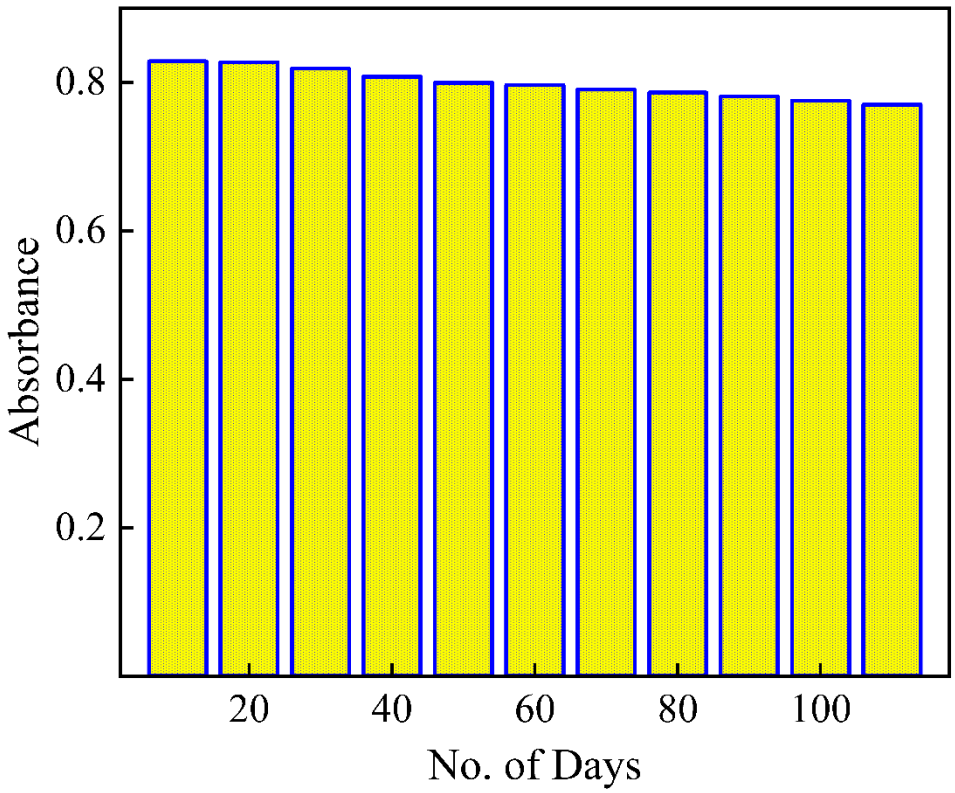

Figure 4.6. Variation of Absorption intensity with No. of Days

4.3. ZETA POTENTIAL ANALYSIS

Zeta potential is a critical factor that influences the stability and morphology of colloidal suspensions [69]. It indicates the nature and magnitude of the charge associated with the particle. Zeta potential in colloidal suspensions denotes electrostatic repulsion between nearby, similar-charged particles [70]. In general, stable suspensions of colloidal nanoparticles are formed when the zeta potential values are more positive or negative than ± 30 mV form. This is due to the inter-particle electrostatic repulsion. The plot in Figure 4.7 displays the distribution of particle sizes for sample S5 with the largest size intensity at 32.7 nm. Thus the average size of synthesized AuNPs is around 32.7 nm and the zeta potential value recorded is -29.6 mV, showing very high stability of the synthesized AuNPs as compared to previously

reported zeta potential values [71]. Dynamic light scattering (DLS) uses the scattered light intensity as a parameter for the measurement of the hydrodynamic diameter of a sample, which possibly explains the increase in average size compared to crystallite size [72].

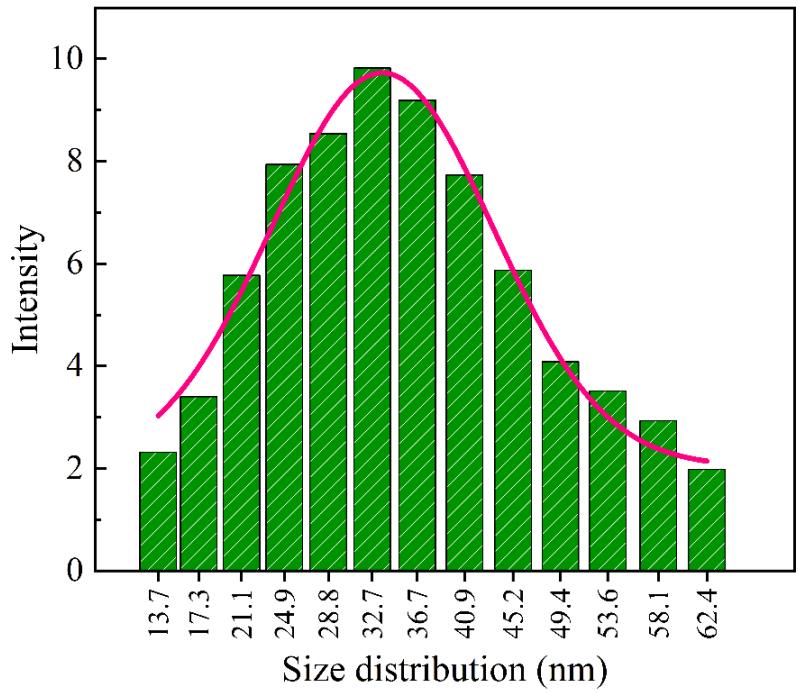

Figure 4.7. Size distribution of colloidal AuNPs obtained from DLS analysis

4.4. HRTEM ANALYSIS

Figure 4.8 shows the HRTEM images at various magnifications of samples S1, S3 and S5. Figure 4.8(a and b) shows the images of sample S1 of biosynthesized AuNPs at magnifications of 20 and 50 nm, respectively, along with the magnification of 5 nm (the inset of a). These images indicate that sample S1 contains particles having different shapes, such as oval and spherical. Figure 4.8(c) illustrates the particle size distribution obtained using HRTEM images with the average size of sample S1 is 53 nm. Figure 4.8(d and e) shows the images for sample S3, indicating that upon

increasing synthesis time, the particles tend to acquire a more symmetrical and uniform shape. Figure 4.8(f) represents the size distribution of S3, which indicates the average particle size for S3 to be 21 nm. With a further increase in synthesis time, the nanoparticles will gain a more uniform and symmetrical shape, as shown in Figures 4.8(g and h), showing spherical gold nanoparticles for sample S5, which is likely due to the increased opportunity for nucleation and growth of the nanoparticles [73]. Figure 4.8(i) illustrates the particle size distribution of S5, indicating an average particle size of AuNPs to be 19 nm, close to crystallite size.

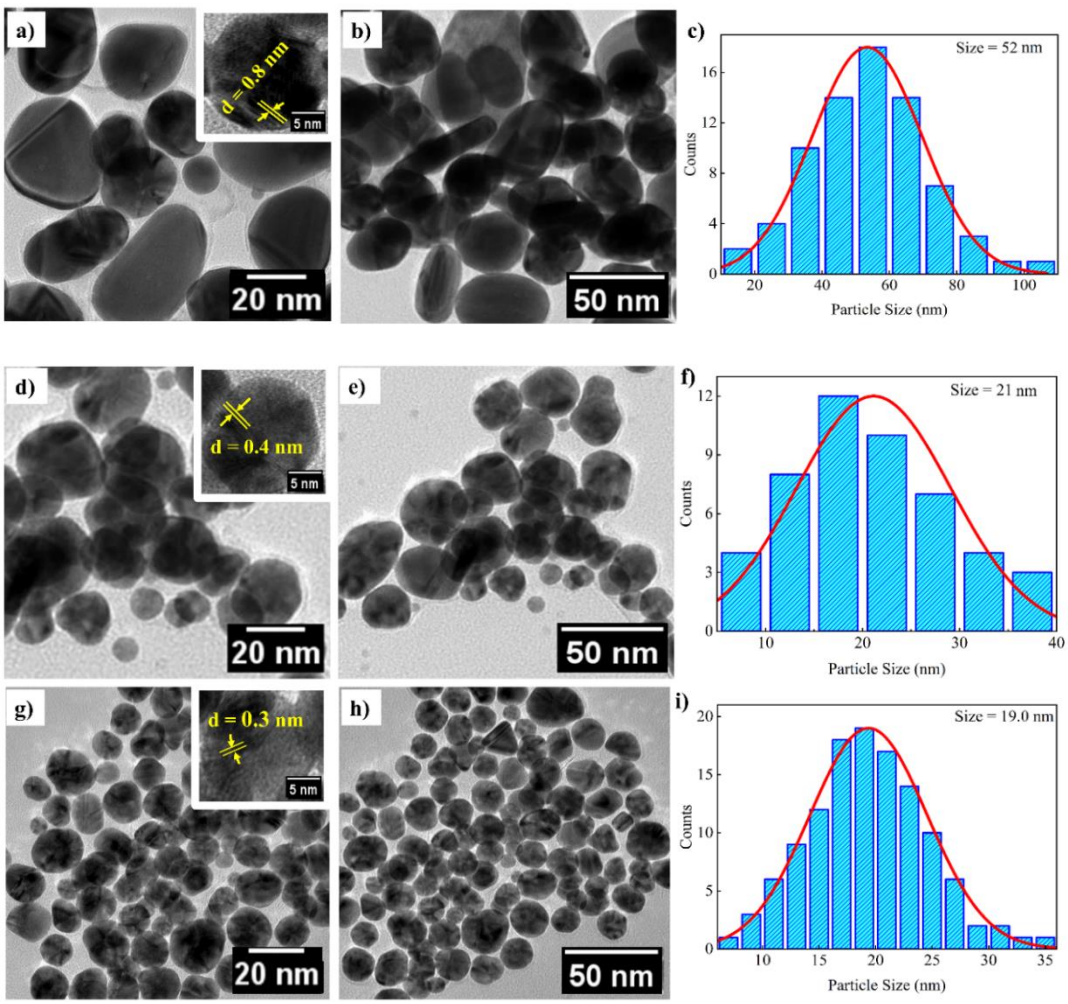

Figure 4.8. HRTEM images at a magnification of 20 and 50 nm along with particle size distribution of S1 (a,b,c), S3 (d, e, f) and S5 (g, h, i), respectively. The inset of (a,d,g) represents the image at a 5 nm magnification.

4.5. FTIR ANALYSIS

The FTIR technique offers a powerful tool for probing the molecular interactions and bonding characteristics of nanoscale materials. By examining the spectral fingerprints obtained from the FTIR analysis, we can gain valuable information about the functional groups present on the surface of the AuNPs, elucidating their stabilization mechanism and overall integrity. FTIR analysis enables the identification of organic compounds, surfactants, or biomolecules that have been involved in the synthesis process, further enhancing the understanding of the green synthesis pathway.

Several phytochemicals and biomolecules have been reported to be present in *Kalanchoe Fedtschenkoi* plant, including organic acids such as malic acid and citric acid, flavonoids such as quercetin and kaempferol, alkaloids such as bufadienolides and glycosides, and polysaccharides [74]. FTIR analysis of gold nanoparticles synthesized using *Kalanchoe Fedtschenkoi* extract was measured to detect different functional groups involved in the formation of AuNPs.

The FTIR spectra of sample S5 and the plant extract are shown in Figure 4.9. The broader peak recorded at 3297 cm^{-1} can be attributed to the vibrations of the hydroxyl (O-H) bond, which indicates presence of alcoholic and phenolic compounds [75] and is also observed in terpene and fatty acids. The band at 1636 cm^{-1} can be due to the stretching vibrations of C=C bonds [76]. The presence of an aromatic component is evident by the weak band observed at 2098 cm^{-1} [77]. The FTIR analysis showed the presence of hydroxyl, carbonyl and carboxyl groups, which are commonly found in flavonoids, organic acids and polysaccharides, which are possibly responsible for the stabilization and reduction of AuNPs.

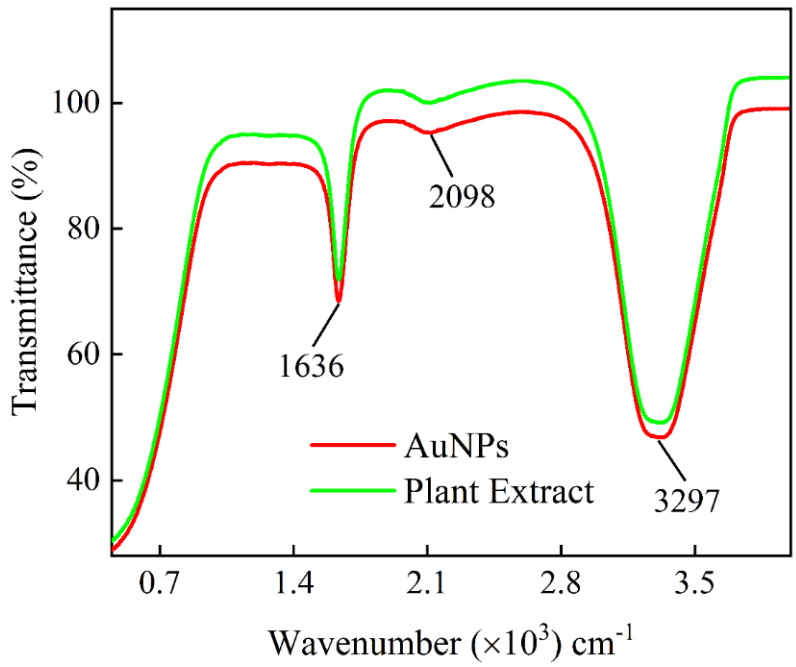

Figure 4.9. FTIR spectra of biosynthesized colloidal AuNPs and plant extract

4.6. INTERACTION WITH BSA

The structure of BSA protein is defined by 583 amino acid residues forming a single polypeptide chain and 17 disulfide links and a single thiol (SH) group. The possible mechanism underlying the interaction of the protein with AuNPs may be passive adsorption [78], in which particular charge functional protein groups are joined to the surface of gold nanoparticles forming covalent or non-covalent interactions. Figure 4.10 shows the pictorial representation of BSA adsorption on AuNPs.

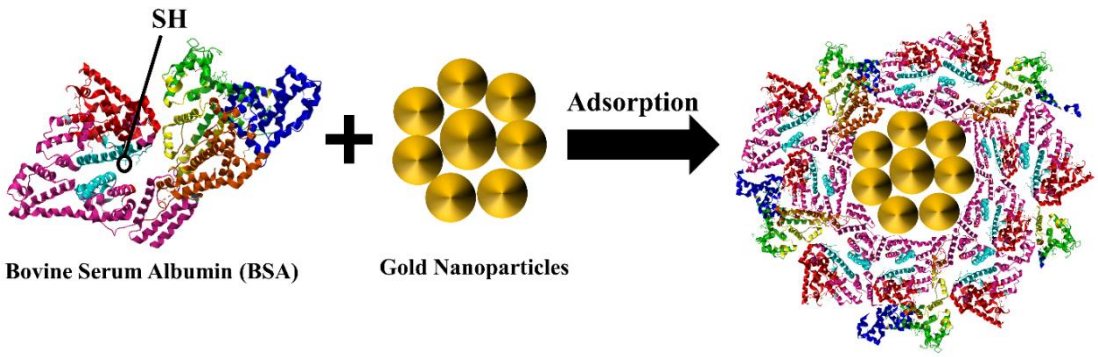

Figure 4.10. Plausible route of adsorption of BSA on AuNPs

In BSA, the thiol (SH) group in the albumin cysteine residues interacts with the Au atoms on the surface of AuNPs, initiating the creation of Au-S covalent bonds. Because BSA contains binding sites, direct adsorption could be accomplished by simply incubating gold nanoparticles with BSA. Figure 4.11 shows the surface diagram of BSA illustrating the interaction of the thiol group of BSA with AuNPs, possibly in the form of adsorption, where the thiol group of BSA binds with the Au atoms present on the surface of the AuNPs, leads to the formation of a stable complex between BSA and AuNPs [79]. The methodological ease and economy of this adsorption strategy, which avoids the employment of extra reagents and extreme conditions, make it exceptional and sustainable.

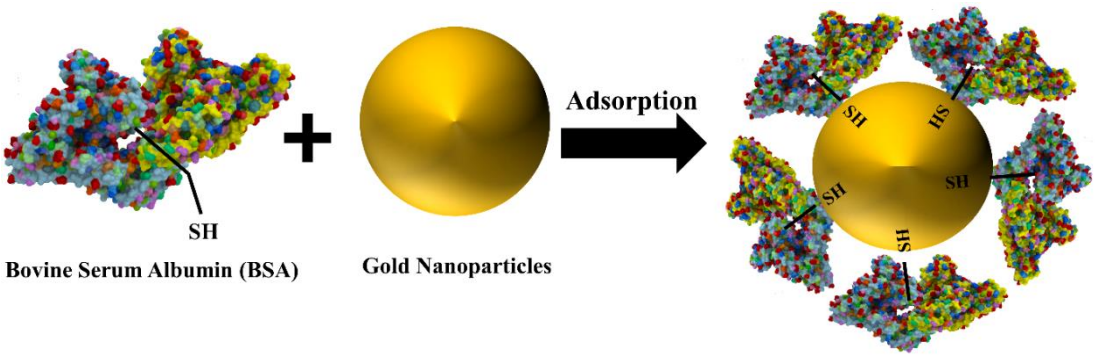

Figure 4.11. Possible interaction of SH group of BSA with AuNPs

4.6.1. Absorption of BSA

The interaction between BSA and AuNPs was examined by measuring the absorption spectra of BSA, along with the increasing concentration of AuNPs from 0.9 to 181 μM. Figure 4.12 shows that BSA has a strong absorption band at 278 nm. The absorption band intensity gradually increases along with the rise in the concentration of AuNPs with no significant shift in absorption maxima. The stable complex in the ground state formed due to interaction between BSA and AuNPs, as the thiol group of

BSA binds with the gold atoms present on the surface of AuNPs, may be the plausible cause of the increase in intensity [80]. As observed, the concentration of AuNPs used has no discernible optical density in the region of BSA absorption spectra; the enhanced BSA absorption is most likely the result of forming a ground-state stable complex due to intermolecular interactions [81].

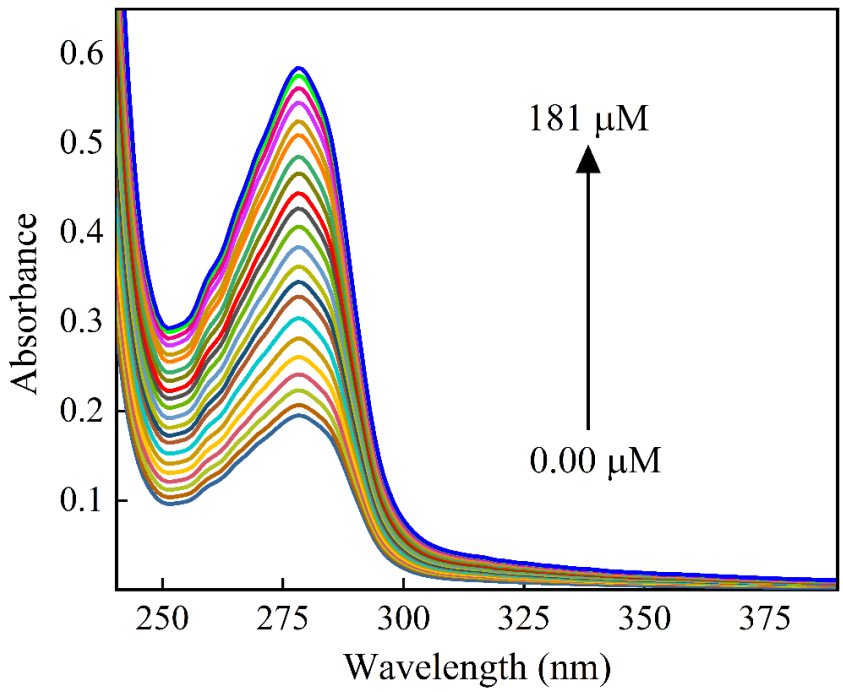

Figure 4.12. Absorption spectra of BSA (0.5 μM) with increasing concentration of colloidal AuNPs

Figure 4.13 illustrates the Benesi-Hildebrand (B-H) absorption plot for increasing the concentration of AuNPs. The binding constant, K_b was determined using the method reported by [82] using Eq. (4.1).

$$\frac{1}{A-A_0} = \frac{1}{A_{co}-A_0} + \frac{1}{K_b(A_{co}-A_0)[Q]} \tag{4.1}$$

where A represents the absorbance of BSA with different concentrations of AuNPs at 278 nm, A_0 and A_{co} indicate the absorbance of BSA at its initial concentration and in

the presence of AuNPs at 278 nm, respectively, and [Q] is the AuNPs concentration in M. The plot of $1/(A - A_0)$ vs. 1/[Q] is linear with a slope that equals to $1/K_b(A_{co} - A_0)$ and intercept, which equals to $1/(A_{co} - A_0)$. The plot showed a linear relation with R^2 = 0.99 with a value of K_b as 4×10^4 M^{-1}, hence shows a strong binding.

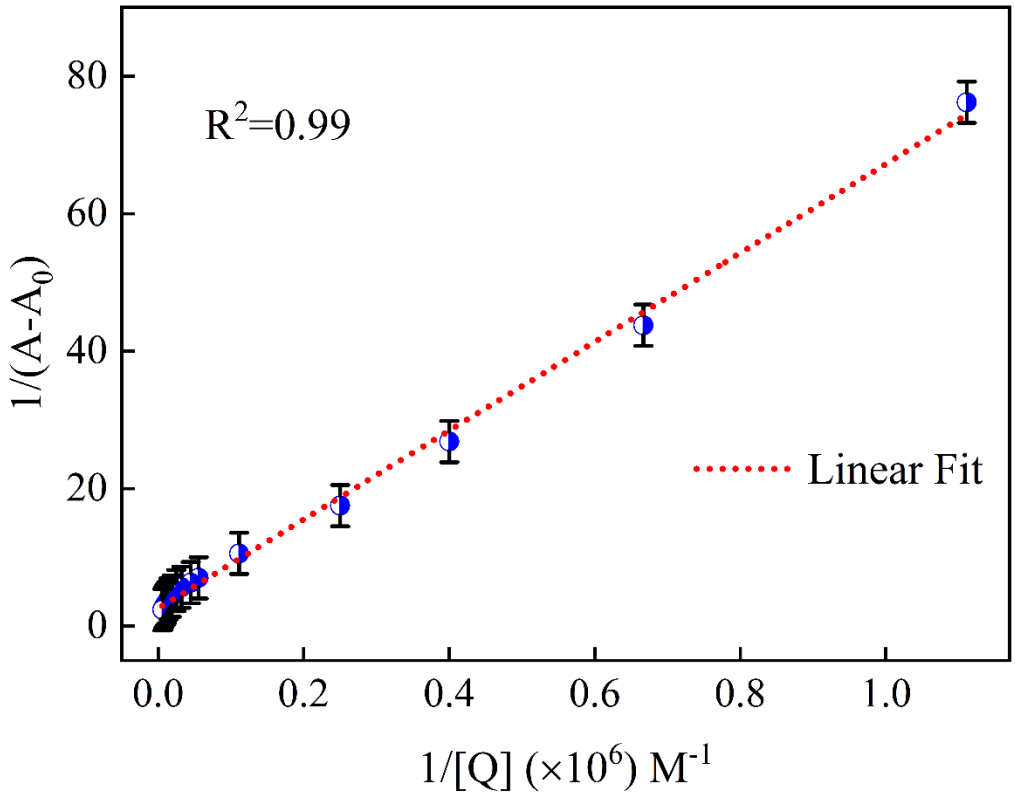

Figure 4.13. Plot (B-H) of $(\frac{1}{A-A_0})$ *vs.* 1/[Q]

4.6.2. Fluorescence of BSA

The interaction of BSA with AuNPs was monitored by measuring the change in fluorescence (FL) intensity, which was quenched by increasing concentrations of AuNPs from 0 to 181 μ M. The strong FL band of BSA at 351 nm is shown in Fig.4.14. In the presence of AuNPs, BSA's FL intensity reduces, indicating that the former interacts with one of the protein's two tryptophan residues (Trp-134 or Trp-213) [83].

It is significant to notice that in the experimental conditions, the BSA's excitation wavelength (280 nm) does not coincide with the SPR peak (525 nm) of AuNPs, demonstrating that the quenching process is carried out by nanoparticles [51]. The thiol group of BSA molecules gets adsorbed on the surface of AuNPs. When the binding site is close to AuNPs, FL mainly from the tryptophan moiety of BSA is quenched, and the free BSA in the solution emits the remaining fluorescence [84]. As an outcome, the un-adsorbed probe molecule of the BSA is responsible for the signal contribution to the FL spectra [52]. The linear Stern-Volmer indicates that there is only one sort of quenching in the system. Considering that internal energy transfer requires a good overlap between the FL and the absorption spectra of the donor and acceptor [51], due to the significant Stokes shift, the resulting overlap between the FL and absorption spectra is insufficient for enabling the energy transfer process.

To investigate the mechanism of quenching, FL intensity was recorded with varying AuNPs concentrations, and the Stern-Volmer (S-V) plot was obtained (Fig. 4.15) with Eq. 4.2 [85].

$$\frac{F_0}{F} = 1 + K_{SV}[Q] \tag{4.2}$$

Where F_0 and F represents BSA's FL intensities in the absence and presence of AuNPs, respectively. The S-V plot revealed a linear relationship between the concentration of AuNPs and FL intensity with $R^2 = 0.99$. K_{SV}, referred to as the S-V constant or the quenching constant, is estimated to be $7.2 \times 10^4\ \mathrm{M}^{-1}$ using Eq. 4.2. The corresponding limit of detection (LoD) for AuNPs was calculated using $3\sigma/\mathrm{K}$ [86], where σ indicates the standard deviation and K is the slope of the plot, to be 6 µM.

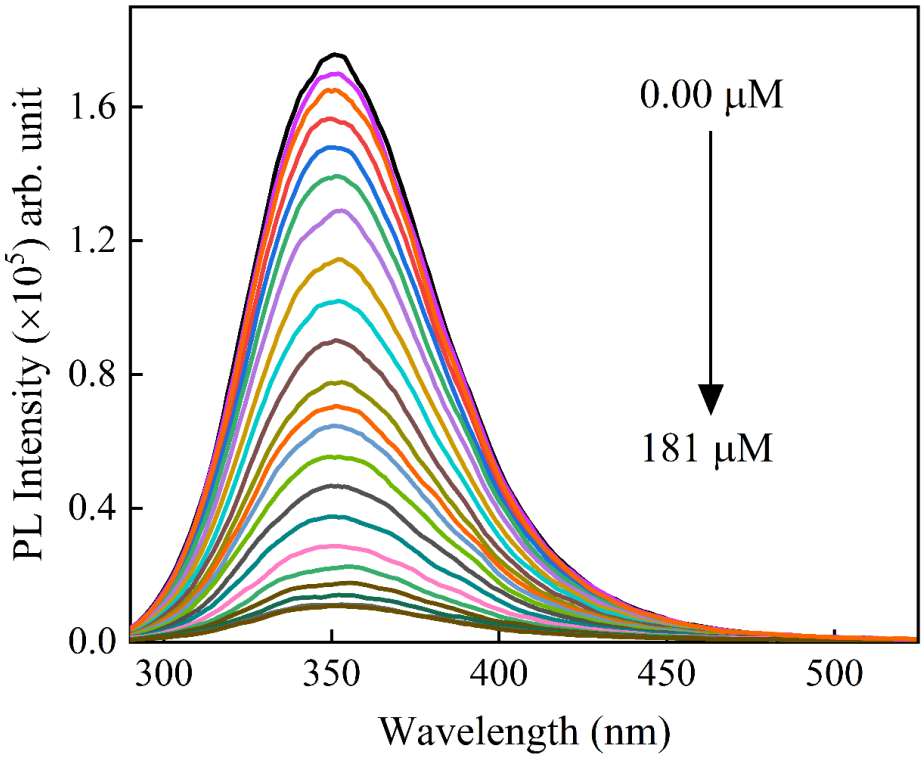

Figure 4.14. Fluorescence spectra of BSA (0.5 μM) with increasing concentration of AuNPs

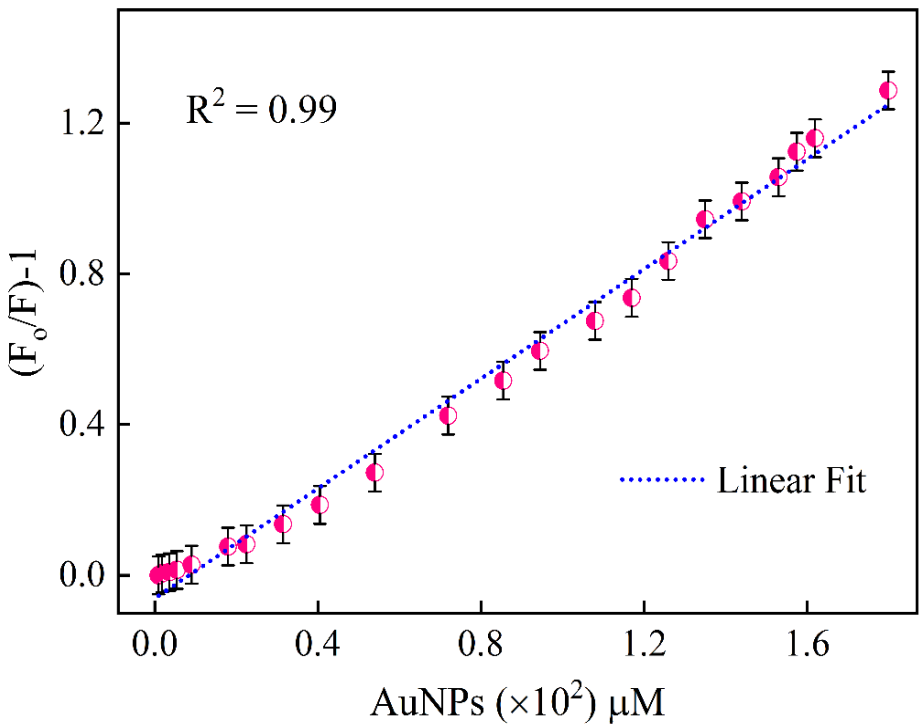

Figure 4.15. The plot of (F_0/F)-1 *vs.* concentration of AuNPs

4.7. CATALYTIC PERFORMANCE OF AuNPs

Additionally, the well-crystalline AuNPs were used for the catalytic reaction and to degrade the textile dye methylene blue (MB) in the presence of a reference and reducing agent, $NaBH_4$. As observed, MB dye deteriorated from a vivid blue to almost colorless after 16 minutes (insets of Fig. 4.16c). Figure 4.16 represents the absorption spectra of methylene blue dye in DI water with $NaBH_4$ in the presence and absence of AuNPs. At approximately 664 nm, MB dye exhibits its distinctive lower energy absorption band, which corresponds to the $n - \pi^*$ transitions [56].

MB is carcinogenic and mutagenic to living things and is toxic in natural water, and its concentration in the body can be hazardous [55]. The absorption intensity was somewhat reduced in the addition of $NaBH_4$ and AuNPs alone (Fig. 4.16(a, b)), demonstrating no discernible color change of MB solutions (insets of Fig. 4.16(a, b)) and the MB dye degraded was 29 % and 18 %, respectively. However, the addition of $NaBH_4$ reduced the amount of MB and stabilized it, which led to a minor decrease in absorption intensity. After adding a modest amount of AuNPs, the absorption intensity reduces steadily and almost entirely after 16 minutes. The absorption intensity is decreased by about 94 %, a point at which the color is lost (Fig. 4.16c). AuNPs act as a charge carrier and initialize a transfer of electrons from nucleophilic BH_4^- ions to electrophilic dye molecules [87], might be a plausible reason for the reduction of MB dye to leucomethylene blue. [55].

AuNPs perform as active catalysts in the reduction of MB dye using $NaBH_4$ by providing a surface for BH_4^- donor ions to get adsorbed [88]. The absorption peak of MB dye arises around 300 nm (not shown), increases initially and decreases

subsequently, which is plausibly due to the overlap of the absorption of plant extract and due to degradation of dye [87]. The presence of AuNPs increases the concentration of active sites, allowing the reaction to occur faster.

However, when used alone, AuNPs and $NaBH_4$ provide electrons for dye reduction reactions, but their combined use is far more efficient. The degradation percentage was calculated using $\left(\frac{A_0 - A_t}{A_0}\right) \times 100\%$, where A_0 and A_t indicates intensities of absorption of dye at 664 nm initially at time t = 0 (pure dye) and at time t, respectively. The rate constant for the degradation of MB dye is calculated using the relation $\ln\left(\frac{A_t}{A_0}\right) = -kt$, where k is the rate constant of reaction and *t* represents the reaction time [56]. The plot of $\ln\left(\frac{A_t}{A_0}\right)$ *vs. t* is given in Fig. 4.16(d), which shows a linear relation, showing the pseudo-first-order reaction kinetics of degradation reaction of MB dye [59]. The rate constant (k) for the degradation of MB dye using AuNPs with sodium borohydride was determined to be 0.175 min^{-1}.

AuNPs with $NaBH_4$ degraded the dye by 94 % in 16 minutes, which is quite faster than the degradation time reported in previous reports [89, 90], hence demonstrating a more efficient catalyst while synthesized using *Kalanchoe Fedtschenkoi* plant. However, a faster rate has also been reported in some reports [55, 91]. This variation and slowness in the reaction rate in the present system can be attributed to the differences in the synthesis approaches, various physiochemical factors, and the concentration and amount of different materials used for the experimental process. Further optimization of these parameters could potentially lead to even faster degradation rates.

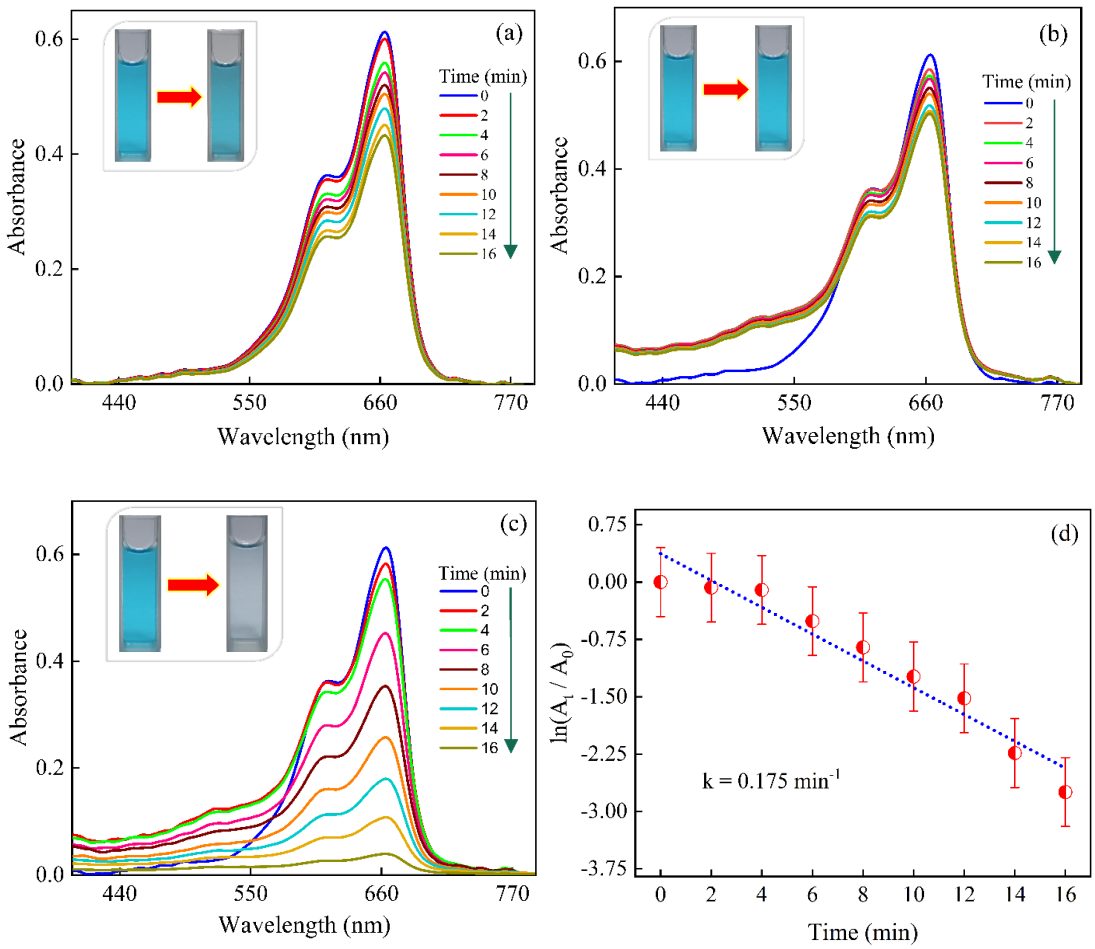

Figure 4.16. Absorption spectra of methylene blue with reaction time in the presence of $NaBH_4$ (a), AuNPs (b) and $NaBH_4$ + AuNPs (c). The plot of $\ln(\frac{A_t}{A_0})$ of MB with $NaBH_4$ + AuNPs as a function of time (d).

CHAPTER 5

CONCLUSION

Highly efficient gold nanoparticles were successfully synthesized using an environmentally-friendly and cost-effective using the leaves of the plant *Kalanchoe Fedtschenkoi*. The morphology and size of produced AuNPs reveal a consistent spherical shape. The AuNPs exhibited excellent crystalline structure having an average particle size of 19 nm. The AuNPs show a strong SPR band at 525 nm. The AuNPs are highly stable and examined with a zeta potential of -29.6 mV and absorption spectra of 4 months since the absorption spectra did not significantly change over time.

Further, interactions of AuNPs and BSA, BSA forms a very important component of plasma which functions as a drug carrier and helps digest fatty acids, was examined by recording the change in absorption and FL intensities of BSA with increasing concentration of AuNPs. The fluorescence intensity of BSA was quenched following the linear S-V relation with LoD of 6 µM. The adsorption of BSA on the surface of AuNPs indicated improved drug transfer properties of BSA and extra stability of AuNPs. Employment of AuNPs degraded textile dye MB remarkably in 16 minutes. 94% of the dye was degraded in the presence of $NaBH_4$ + AuNPs, while degraded only by 29 % and 18% in the presence of $NaBH_4$ and AuNPs, respectively. In addition, AuNPs have potential applications in areas such as antibacterial, antifungal, antioxidant, antimicrobial and anticancer properties.

The graphical abstract shown in Fig. 5.1 encapsulate the crucial aspects of this research, including the synthesis procedure, characterizations, and outcomes of the interaction of AuNPs with BSA and the catalytic properties.

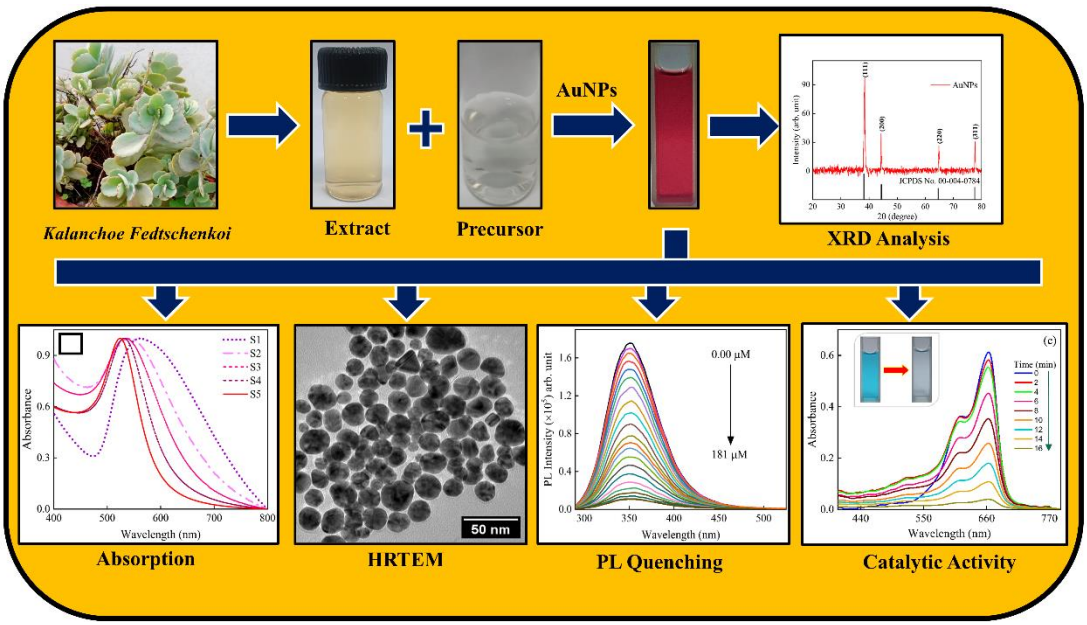

Figure 5.1. Graphical Abstract

RESEARCH PAPER

Published article "A Sustainable Approach to Develop Gold Nanoparticles with *Kalanchoe Fedtschenkoi* and Their Interaction with Protein and Dye: Sensing and Catalytic Probe"

SpringerLink Search Log in

Home > Plasmonics > Article

Published: 09 March 2023

A Sustainable Approach to Develop Gold Nanoparticles with *Kalanchoe fedtschenkoi* and Their Interaction with Protein and Dye: Sensing and Catalytic Probe

Neha Bhatt & Mohan Singh Mehata

Plasmonics (2023) | Cite this article

Abstract

In this study, highly stable gold nanoparticles (AuNPs) of different sizes ranging from 15 to 55 nm were synthesized via an eco-friendly, sustainable, and cost-efficient approach using a specific plant, *Kalanchoe fedtschenkoi*. The AuNPs demonstrated an absorption maximum at around 525 nm, hence exhibiting a strong surface plasmon resonance (SPR) band that is created when the free electrons of the AuNPs oscillate in harmony with the frequency of incident light. The impact of physiochemical environments, pH, and temperature was examined. The crystal structure and stability of the produced AuNPs were validated with an X-ray diffractogram, zeta potential analysis, and absorption. The morphology, structure, and bonds were examined using HRTEM and FTIR, respectively. The interaction of AuNPs (concentrations range of 0–181 μM) with plasma protein bovine serum albumin was explored using absorption and fluorescence studies. Furthermore, AuNPs were utilized as an active catalyst for the degradation of dye methylene blue (MB) in the presence of $NaBH_4$. MB was degraded by 94%, and the solution became colorless within 16 min with a rate constant of 0.175 min^{-1}.

Sections | Figures | References

REFERENCES

[1] S. Jain and M. S. Mehata, “Medicinal Plant Leaf Extract and Pure Flavonoid Mediated Green Synthesis of Silver Nanoparticles and their Enhanced Antibacterial Property,” *Sci. Rep.*, vol. 7, no. 1, p. 15867, 2017, doi: 10.1038/s41598-017-15724-8.

[2] N. Dasgupta, S. Ranjan, and C. Ramalingam, “Applications of nanotechnology in agriculture and water quality management,” *Environ. Chem. Lett.*, vol. 15, no. 4, pp. 591–605, 2017, doi: 10.1007/s10311-017-0648-9.

[3] R. Geetha, T. Ashokkumar, S. Tamilselvan, K. Govindaraju, M. Sadiq, and G. Singaravelu, “Green synthesis of gold nanoparticles and their anticancer activity,” *Cancer Nanotechnol.*, vol. 4, no. 4–5, pp. 91–98, 2013, doi: 10.1007/s12645-013-0040-9.

[4] M. Das, K. H. Shim, S. S. A. An, and D. K. Yi, “Review on gold nanoparticles and their applications,” *Toxicol. Environ. Health Sci.*, vol. 3, no. 4, pp. 193–205, 2011, doi: 10.1007/s13530-011-0109-y.

[5] K. Perveen *et al.*, “Microwave-assisted rapid green synthesis of gold nanoparticles using seed extract of trachyspermum ammi: Ros mediated biofilm inhibition and anticancer activity,” *Biomolecules*, vol. 11, no. 2, p. 197, 2021, doi: 10.3390/biom11020197.

[6] A. G. Kolhatkar, A. C. Jamison, D. Litvinov, R. C. Willson, and T. R. Lee, "Tuning the magnetic properties of nanoparticles," *Int. J. Mol. Sci*, vol. 14, no. 8, pp. 15977-16009, 2013.

[7] A. Umer, S. Naveed, N. Ramzan, and M. S. Rafique, “Selection of a suitable method for the synthesis of copper nanoparticles,” *Nano*, vol. 7, no. 5, p. 1230005, 2012, doi: 10.1142/S1793292012300058.

[8] V. Anand and V. C. Srivastava, “Zinc oxide nanoparticles synthesis by electrochemical method: Optimization of parameters for maximization of productivity and characterization,” *J. Alloys Compd.*, vol. 636, pp. 288–292,

2015, doi: 10.1016/j.jallcom.2015.02.189.

[9] C. C. Lin and Y. L. Wei, “Enhanced reactivity of copper nanoparticles mass-produced by reductive precipitation in a rotating packed bed with blade packings,” *J. Mater. Res. Technol.*, vol. 9, no. 6, pp. 12328–12334, 2020, doi: 10.1016/j.jmrt.2020.08.080.

[10] N. Silva, S. Ramírez, I. Díaz, A. Garcia, and N. Hassan, “Easy, quick, and reproducible sonochemical synthesis of CuO nanoparticles,” *Materials (Basel).*, vol. 12, no. 5, p. 804, 2019, doi: 10.3390/MA12050804.

[11] P. M. Aneesh, K. A. Vanaja, and M. K. Jayaraj, “Synthesis of ZnO nanoparticles by hydrothermal method,” *Nanophotonic Mater. IV*, vol. 6639, p. 66390J, 2007, doi: 10.1117/12.730364.

[12] V. C. Téllez *et al.*, “Green synthesis of palladium mixed with PdO nanoparticles by chemical bath deposition,” *Opt. Mater. (Amst).*, vol. 112, p. 110747, 2021, doi: 10.1016/j.optmat.2020.110747.

[13] C. Daruich De Souza, B. Ribeiro Nogueira, and M. E. C. M. Rostelato, “Review of the methodologies used in the synthesis gold nanoparticles by chemical reduction,” *J. Alloys Compd.*, vol. 798, pp. 714–740, 2019, doi: 10.1016/j.jallcom.2019.05.153.

[14] P. Lassègue, L. Noé, M. Monthioux, and B. Caussat, “Fluidized bed chemical vapor deposition of copper nanoparticles on multi-walled carbon nanotubes,” *Surf. Coatings Technol.*, vol. 331, pp. 129–136, 2017, doi: 10.1016/j.surfcoat.2017.10.046.

[15] B. R. Gangapuram, R. Bandi, M. Alle, R. Dadigala, G. M. Kotu, and V. Guttena, “Microwave assisted rapid green synthesis of gold nanoparticles using Annona squamosa L peel extract for the efficient catalytic reduction of organic pollutants,” *J. Mol. Struct.*, vol. 1167, pp. 305–315, 2018, doi: 10.1016/j.molstruc.2018.05.004.

[16] J. Virkutyte and R. S. Varma, “Green synthesis of nanomaterials:

Environmental aspects," *ACS Symp. Ser.*, vol. 1124, pp. 11–39, 2013, doi: 10.1021/bk-2013-1124.ch002.

[17] P. Sheth, H. Sandhu, D. Singhal, W. Malick, N. Shah, and M. Serpil Kislalioglu, "Nanoparticles in the Pharmaceutical Industry and the Use of Supercritical Fluid Technologies for Nanoparticle Production," *Curr. Drug Deliv.*, vol. 9, no. 3, pp. 269–284, 2012, doi: 10.2174/156720112800389052.

[18] M. Nasrollahzadeh, M. Sajjadi, S. Iravani, and R. S. Varma, "Green-synthesized nanocatalysts and nanomaterials for water treatment: Current challenges and future perspectives," *J. Hazard. Mater.*, vol. 401, p. 123401, 2021, doi: 10.1016/j.jhazmat.2020.123401.

[19] M. Shakibaie *et al.*, " Green synthesis of gold nanoparticles by the marine microalga Tetraselmis suecica ," *Biotechnol. Appl. Biochem.*, vol. 57, no. 2, pp. 71–75, 2010, doi: 10.1042/ba20100196.

[20] P. Mukherjee *et al.*, "Potential therapeutic application of gold nanoparticles in B-chronic lymphocytic leukemia (BCLL): Enhancing apoptosis," *J. Nanobiotechnology*, vol. 5, p. 4, 2007, doi: 10.1186/1477-3155-5-4.

[21] G. A. Petkova, K. Záruba, P. Žvátora, and V. Král, "Gold and silver nanoparticles for biomolecule immobilization and enzymatic catalysis," *Nanoscale Res. Lett.*, vol. 7, p. 287, 2012, doi: 10.1186/1556-276X-7-287.

[22] S. Zeng, K. T. Yong, I. Roy, X. Q. Dinh, X. Yu, and F. Luan, "A Review on Functionalized Gold Nanoparticles for Biosensing Applications," *Plasmonics*, vol. 6, no. 3, pp. 491–506, 2011, doi: 10.1007/s11468-011-9228-1.

[23] Weibo Cai, Ting Gao, Hao Hong, J. Sun, "Applications of gold nanoparticles in cancer nanotechnology," *Nanotechnol. Sci. Appl.*, vol. 1, pp. 17–32, 2008, doi: 10.4018/978-1-5225-3158-6.ch035.

[24] S. Sathiyaraj *et al.*, "Biosynthesis, characterization, and antibacterial activity of gold nanoparticles," *J. Infect. Public Health*, vol. 14, no. 12, pp. 1842–1847, 2021, doi: 10.1016/j.jiph.2021.10.007.

[25] Y. Zhang, T. P. Shareena Dasari, H. Deng, and H. Yu, "Antimicrobial Activity of Gold Nanoparticles and Ionic Gold," *J. Environ. Sci. Heal. - Part C Environ. Carcinog. Ecotoxicol. Rev.*, vol. 33, no. 3, pp. 286–327, 2015, doi: 10.1080/10590501.2015.1055161.

[26] C. T. Beales and O. Medalia, "Gold nanomaterials and their potential use as cryo-electron tomography labels," *J. Struct. Biol.*, vol. 214, no. 3, p. 107880, 2022, doi: 10.1016/j.jsb.2022.107880.

[27] H. Jans and Q. Huo, "Gold nanoparticle-enabled biological and chemical detection and analysis," *Chem. Soc. Rev.*, vol. 41, no. 7, pp. 2849–2866, 2012, doi: 10.1039/c1cs15280g.

[28] M. Shkir *et al.*, "A facile synthesis of Au-nanoparticles decorated PbI_2 single crystalline nanosheets for optoelectronic device applications," *Sci. Rep.*, vol. 8, no. 1, p. 13806, 2018, doi: 10.1038/s41598-018-32038-5.

[29] T. A. El-Brolossy *et al.*, "Shape and size dependence of the surface plasmon resonance of gold nanoparticles studied by Photoacoustic technique," *Eur. Phys. J. Spec. Top.*, vol. 153, no. 1, pp. 361–364, 2008, doi: 10.1140/epjst/e2008-00462-0.

[30] A. García-Quintero and M. Palencia, "A critical analysis of environmental sustainability metrics applied to green synthesis of nanomaterials and the assessment of environmental risks associated with the nanotechnology," *Sci. Total Environ.*, vol. 793, p. 148524, 2021, doi: 10.1016/j.scitotenv.2021.148524.

[31] M. Khalaj, M. Kamali, M. E. V. Costa, and I. Capela, "Green synthesis of nanomaterials - A scientometric assessment," *J. Clean. Prod.*, vol. 267, p. 122036, 2020, doi: 10.1016/j.jclepro.2020.122036.

[32] K. P. Kumar, W. Paul, and C. P. Sharma, "Green synthesis of gold nanoparticles with Zingiber officinale extract: Characterization and blood compatibility," *Process Biochem.*, vol. 46, no. 10, pp. 2007–2013, 2011, doi: 10.1016/j.procbio.2011.07.011.

[33] D. Philip, “Honey mediated green synthesis of gold nanoparticles,” *Spectrochim. Acta - Part A Mol. Biomol. Spectrosc.*, vol. 73, no. 4, pp. 650–653, 2009, doi: 10.1016/j.saa.2009.03.007.

[34] D. Philip, C. Unni, S. A. Aromal, and V. K. Vidhu, “Murraya Koenigii leaf-assisted rapid green synthesis of silver and gold nanoparticles,” *Spectrochim. Acta - Part A Mol. Biomol. Spectrosc.*, vol. 78, no. 2, pp. 899–904, 2011, doi: 10.1016/j.saa.2010.12.060.

[35] M. Noruzi, D. Zare, K. Khoshnevisan, and D. Davoodi, “Rapid green synthesis of gold nanoparticles using Rosa hybrida petal extract at room temperature,” *Spectrochim. Acta - Part A Mol. Biomol. Spectrosc.*, vol. 79, no. 5, pp. 1461–1465, 2011, doi: 10.1016/j.saa.2011.05.001.

[36] S. A. Aromal, V. K. Vidhu, and D. Philip, “Green synthesis of well-dispersed gold nanoparticles using Macrotyloma uniflorum,” *Spectrochim. Acta - Part A Mol. Biomol. Spectrosc.*, vol. 85, no. 1, pp. 99–104, 2012, doi: 10.1016/j.saa.2011.09.035.

[37] D. G. Sant *et al.*, “ Adiantum philippense L. Frond Assisted Rapid Green Synthesis of Gold and Silver Nanoparticles ,” *J. Nanoparticles*, vol. 2013, pp. 1–9, 2013, doi: 10.1155/2013/182320.

[38] N. Ahmad, S. Sharma, and R. Rai, “Rapid green synthesis of silver and gold nanoparticles using peels of Punica granatum,” *Adv. Mater. Lett.*, vol. 3, no. 5, pp. 376–380, 2012, doi: 10.5185/amlett.2012.6357.

[39] P. Elia, R. Zach, S. Hazan, S. Kolusheva, Z. Porat, Y. Zeiri, “Green synthesis of gold nanoparticles using plant extracts as reducing agents,” *Int. J. Nanomedicine*, vol. 9, no. 1, pp. 4007–4021, 2014, doi: 10.2147/IJN.S57343.

[40] C. Wang *et al.*, “Rapid green synthesis of silver and gold nanoparticles using Dendropanax morbifera leaf extract and their anticancer activities,” *Int. J. Nanomedicine*, vol. 11, pp. 3691–3701, 2016, doi: 10.2147/IJN.S97181.

[41] A. Hatipoğlu, “Rapid green synthesis of gold nanoparticles: Synthesis,

characterization, and antimicrobial activities," *Prog. Nutr.*, vol. 23, no. 3, p. e2021242, 2021, doi: 10.23751/pn.v23i3.11988.

[42] N. Gogoi and U. Bora, "Green synthesis of gold nanoparticles using Nyctanthes arbortristis flower extract," *Bioprocess Biosyst Eng*, vol. 34, pp. 615–619, 2011, doi: 10.1007/s00449-010-0510-y.

[43] T. Y. Suman, S. R. Radhika Rajasree, R. Ramkumar, C. Rajthilak, and P. Perumal, "The Green synthesis of gold nanoparticles using an aqueous root extract of Morinda citrifolia L," *Spectrochim. Acta - Part A Mol. Biomol. Spectrosc.*, vol. 118, pp. 11–16, 2014, doi: 10.1016/j.saa.2013.08.066.

[44] S. Aswathy Aromal and D. Philip, "Green synthesis of gold nanoparticles using Trigonella foenum-graecum and its size-dependent catalytic activity," *Spectrochim. Acta - Part A Mol. Biomol. Spectrosc.*, vol. 97, pp. 1–5, 2012, doi: 10.1016/j.saa.2012.05.083.

[45] G. F. Smith and E. Figueiredo, "Kalanchoe fedtschenkoi Raym.-Hamet & H.Perrier (Crassulaceae) is spreading in South Africa's Klein Karoo," *Bradleya*, vol. 35, no. 35, pp. 80–86, 2017, doi: 10.25223/brad.n35.2017.a7.

[46] N. Richwagen, J. T. Lyles, B. L. F. Dale, and C. L. Quave, "Antibacterial Activity of Kalanchoe mortagei and K. Fedtschenkoi Against ESKAPE Pathogens," *Front. Pharmacol.*, vol. 10, p. 67, 2019, doi: 10.3389/fphar.2019.00067.

[47] M. Iosin, V. Canpean, and S. Astilean, "Spectroscopic studies on pH- and thermally induced conformational changes of Bovine Serum Albumin adsorbed onto gold nanoparticles," *J. Photochem. Photobiol. A Chem.*, vol. 217, no. 2–3, pp. 395–401, 2011, doi: 10.1016/j.jphotochem.2010.11.012.

[48] N. Wangoo, C. R. Suri, and G. Shekhawat, "Interaction of gold nanoparticles with protein: A spectroscopic study to monitor protein conformational changes," *Appl. Phys. Lett.*, vol. 92, no. 13, p. 133104, 2008, doi: 10.1063/1.2902302.

[49] Y. Ding, Z. Chen, J. Xie, and R. Guo, “Comparative studies on adsorption behavior of thionine on gold nanoparticles with different sizes,” *J. Colloid Interface Sci.*, vol. 327, no. 1, pp. 243–250, 2008, doi: 10.1016/j.jcis.2008.07.057.

[50] P. Roach, D. Farrar, and C. C. Perry, “Interpretation of protein adsorption: Surface-induced conformational changes,” *J. Am. Chem. Soc.*, vol. 127, no. 22, pp. 8168–8173, 2005, doi: 10.1021/ja042898o.

[51] S. Pramanik, P. Banerjee, A. Sarkar, and S. C. Bhattacharya, “Size-dependent interaction of gold nanoparticles with transport protein: A spectroscopic study,” *J. Lumin.*, vol. 128, no. 12, pp. 1969–1974, 2008, doi: 10.1016/j.jlumin.2008.06.008.

[52] B. Bisht, P. Dey, A. K. Singh, S. Pant, and M. S. Mehata, “Spectroscopic investigation on the interaction of direct yellow-27 with protein (BSA),” *Methods Appl. Fluoresc.*, vol. 10, no. 4, p. 044009, 2022, doi: 10.1088/2050-6120/ac8a8b.

[53] S. Ariyasu, H. Hayashi, B. Xing, and S. Chiba, “Site-Specific Dual Functionalization of Cysteine Residue in Peptides and Proteins with 2-Azidoacrylates,” *Bioconjug. Chem.*, vol. 28, no. 4, pp. 897–902, 2017, doi: 10.1021/acs.bioconjchem.7b00024.

[54] O. A. Chaves *et al.*, “Studies of the interaction between bsa and a plumeran indole alkaloid isolated from the stem bark of aspidosperma cylindrocarpon (Apocynaceae),” *J. Braz. Chem. Soc.*, vol. 28, no. 7, pp. 1229–1236, 2017, doi: 10.21577/0103-5053.20160285.

[55] B. Kim, W. C. Song, S. Y. Park, and G. Park, “Green synthesis of silver and gold nanoparticles via sargassum serratifolium extract for catalytic reduction of organic dyes,” *Catalysts*, vol. 11, no. 3, p. 347, 2021, doi: 10.3390/catal11030347.

[56] M. S. Mehata, “Green route synthesis of silver nanoparticles using plants/ginger extracts with enhanced surface plasmon resonance and degradation of textile

dye," *Mater. Sci. Eng. B*, vol. 273, no. May, p. 115418, 2021, doi: 10.1016/j.mseb.2021.115418.

[57] H. Y. Chai, S. M. Lam, and J. C. Sin, "Green synthesis of magnetic Fe-doped ZnO nanoparticles via Hibiscus rosa-sinensis leaf extracts for boosted photocatalytic, antibacterial and antifungal activities," *Mater. Lett.*, vol. 242, pp. 103–106, 2019, doi: 10.1016/j.matlet.2019.01.116.

[58] P. C. L. Muraro *et al.*, "Iron oxide nanocatalyst with titanium and silver nanoparticles: Synthesis, characterization and photocatalytic activity on the degradation of Rhodamine B dye," *Sci. Rep.*, vol. 10, no. 1, p. 3055, 2020, doi: 10.1038/s41598-020-59987-0.

[59] N. Y. Nadaf and S. S. Kanase, "Biosynthesis of gold nanoparticles by Bacillus marisflavi and its potential in catalytic dye degradation," *Arab. J. Chem.*, vol. 12, no. 8, pp. 4806–4814, 2019, doi: 10.1016/j.arabjc.2016.09.020.

[60] Ruby, Aryan, and M. S. Mehata, "Surface plasmon resonance allied applications of silver nanoflowers synthesized from Breynia vitis-idaea leaf extract," *Dalt. Trans.*, vol. 51, no. 7, pp. 2726–2736, 2022, doi: 10.1039/D1DT03592D.

[61] N. T. K. Thanh, N. Maclean, and S. Mahiddine, "Mechanisms of Nucleation and Growth of Nanoparticles in Solution," *Chem. Rev.*, vol. 114, no. 1, pp. 7610–7630, 2014, doi: 10.1021/cr400544s.

[62] S. Rajeshkumar, "Anticancer activity of eco-friendly gold nanoparticles against lung and liver cancer cells," *J. Genet. Eng. Biotechnol.*, vol. 14, no. 1, pp. 195–202, 2016, doi: 10.1016/j.jgeb.2016.05.007.

[63] S. Krishnamurthy, A. Esterle, N. C. Sharma, and S. V. Sahi, "Yucca-derived synthesis of gold nanomaterial and their catalytic potential," *Nanoscale Res. Lett.*, vol. 9, no. 1, p. 627, 2014, doi: 10.1186/1556-276X-9-627.

[64] M. M. H. Khalil, E. H. Ismail, and F. El-Magdoub, "Biosynthesis of Au nanoparticles using olive leaf extract. 1st Nano Updates," *Arab. J. Chem.*, vol.

5, no. 4, pp. 431–437, 2012, doi: 10.1016/j.arabjc.2010.11.011.

[65] D. Philip, “Green synthesis of gold and silver nanoparticles using Hibiscus rosa sinensis,” *Phys. E Low-Dimensional Syst. Nanostructures*, vol. 42, no. 5, pp. 1417–1424, 2010, doi: 10.1016/j.physe.2009.11.081.

[66] V. R. A. Holm, M. M. Greve, and B. Holst, “Temperature induced color change in gold nanoparticle arrays : Investigating the annealing effect on the localized surface plasmon resonance,” *J. Vac. Sci. Technol. B*, vol. 501, p. 06K501, 2016, doi: 10.1116/1.4963153.

[67] A. Dutta and A. Chattopadhyay, “The e ff ect of temperature on the aggregation kinetics of partially bare gold nanoparticles,” *RSC Adv.*, vol. 6, pp. 82138–82149, 2016, doi: 10.1039/c6ra17561a.

[68] S. Yi *et al.*, “Bio-synthesis of gold nanoparticles using English ivy (hedera helix),” *J. Nanosci. Nanotechnol.*, vol. 13, no. 3, pp. 1649–1659, 2013, doi: 10.1166/jnn.2013.7183.

[69] A. Sankhla, R. Sharma, R. Singh, and D. Kashyap, “Biosynthesis and characterization of cadmium sulfide nanoparticles - An emphasis of zeta potential behavior due to capping,” *Mater. Chem. Phys.*, vol. 170, pp. 44–51, 2016, doi: 10.1016/j.matchemphys.2015.12.017.

[70] Aryan, Ruby, and M. S. Mehata, “Green synthesis of silver nanoparticles using Kalanchoe pinnata leaves (life plant) and their antibacterial and photocatalytic activities,” *Chem. Phys. Lett.*, vol. 778, no. May, p. 138760, 2021, doi: 10.1016/j.cplett.2021.138760.

[71] H. Shabestarian *et al.*, “Green synthesis of gold nanoparticles using sumac aqueous extract and their antioxidant activity,” *Mater. Res.*, vol. 20, no. 1, pp. 264–270, 2017, doi: 10.1590/1980-5373-MR-2015-0694.

[72] B. Akbari, M. P. Tavandashti, and M. Zandrahimi, “Particle size characterization of nanoparticles- a practical approach,” *Iran. J. Mater. Sci. Eng.*, vol. 8, no. 2, pp. 48–56, 2011, URL: http://ijmse.iust.ac.ir/article-1-341-

en.html.

[73] R. A. Sperling, P. R. Gil, F. Zhang, M. Zanella, and W. J. Parak, “Biological applications of gold nanoparticles,” *Chem. Soc. Rev.*, vol. 37, no. 9, pp. 1896–1908, 2008, doi: 10.1039/b712170a.

[74] H. C. Huang *et al.*, “Cardenolides and bufadienolide glycosides from Kalanchoe tubiflora and evaluation of cytotoxicity,” *Planta Med.*, vol. 79, no. 14, pp. 1362–1369, 2013, doi: 10.1055/s-0033-1350646.

[75] T. Ahmad, M. Irfan, and S. Bhattacharjee, “Parametric Study on Gold Nanoparticle Synthesis Using Aqueous Elaise Guineensis (Oil palm) Leaf Extract : Effect of Precursor Concentration,” *Procedia Eng.*, vol. 148, pp. 1396–1401, 2016, doi: 10.1016/j.proeng.2016.06.558.

[76] P. Khademi-azandehi and J. Moghaddam, “Green synthesis, characterization and physiological stability of gold nanoparticles from Stachys lavandulifolia Vahl extract,” *Particuology*, vol. 19, pp. 22–26, 2014, doi: 10.1016/j.partic.2014.04.007.

[77] A. Folorunso *et al.*, “Biosynthesis, characterization and antimicrobial activity of gold nanoparticles from leaf extracts of Annona muricata,” *J. Nanostructure Chem.*, vol. 9, no. 2, pp. 111–117, 2019, doi: 10.1007/s40097-019-0301-1.

[78] K. Bolaños, M. J. Kogan, and E. Araya, “Capping gold nanoparticles with albumin to improve their biomedical properties,” *Int. J. Nanomedicine*, vol. 14, pp. 6387–6406, 2019, doi: 10.2147/IJN.S210992.

[79] O. Awotunde, S. Okyem, R. Chikoti, and J. D. Driskell, “Role of Free Thiol on Protein Adsorption to Gold Nanoparticles,” *Langmuir*, vol. 36, no. 31, pp. 9241–9249, 2020, doi: 10.1021/acs.langmuir.0c01550.

[80] H. Alsamamra, I. Hawwarin, S. A. Sharkh, and M. Abuteir, “Study the Interaction between Gold Nanoparticles and Bovine Serum Albumin: Spectroscopic Approach,” *J. Bioanal. Biomed.*, vol. 10, no. 2, pp. 43–49, 2018, doi: 10.4172/1948-593x.1000203.

[81] S. Roy and T. K. Das, “Interaction of biosynthesized gold nanoparticles with BSA and CTDNA: A multi-spectroscopic approach,” *Polyhedron*, vol. 115, pp. 111–118, 2016, doi: 10.1016/j.poly.2016.05.002.

[82] G. Singh *et al.*, “Schiff base-functionalized silatrane-based receptor as a potential chemo-sensor for the detection of Al^{3+} ions,” *New J. Chem.*, vol. 45, no. 17, pp. 7850–7859, 2021, doi: 10.1039/d1nj00943e.

[83] F. Samari, B. Hemmateenejad, M. Shamsipur, M. Rashidi, and H. Samouei, “Affinity of two novel five-coordinated anticancer Pt(II) complexes to human and bovine serum albumins: A spectroscopic approach,” *Inorg. Chem.*, vol. 51, no. 6, pp. 3454–3464, 2012, doi: 10.1021/ic202141g.

[84] S. H. Brewer, W. R. Glomm, M. C. Johnson, M. K. Knag, and S. Franzen, “Probing BSA binding to citrate-coated gold nanoparticles and surfaces,” *Langmuir*, vol. 21, no. 20, pp. 9303–9307, 2005, doi: 10.1021/la050588t.

[85] Aneesha, N. Ohta, and M. S. Mehata, “In situ synthesis of WS_2 QDs for sensing of H_2O_2: Quenching and recovery of absorption and photoluminescence,” *Mater. Today Commun.*, vol. 34, p. 105013, 2023, doi: 10.1016/j.mtcomm.2022.105013.

[86] T. Sun, Y. Su, M. Sun, and Y. Lv, “Homologous chemiluminescence resonance energy transfer on the interface of WS_2 quantum dots for monitoring photocatalytic H_2O_2 evaluation,” *Microchem. J.*, vol. 168, p. 106344, 2021, doi: 10.1016/j.microc.2021.106344.

[87] S. Shukla, A. Masih, Aryan, and M. S. Mehata, “Catalytic activity of silver nanoparticles synthesized using Crinum asiaticum (Sudarshan) leaf extract,” *Mater. Today Proc.*, vol. 56, pp. 3714–3720, 2022, doi: 10.1016/j.matpr.2021.12.468.

[88] P. Saikia, A. T. Miah, and P. P. Das, “Highly efficient catalytic reductive degradation of various organic dyes by Au/CeO_2-TiO_2 nano-hybrid,” *J. Chem. Sci.*, vol. 129, no. 1, pp. 81–93, 2017, doi: 10.1007/s12039-016-1203-0.

[89] M. A. Rabeea, M. N. Owaid, A. A. Aziz, M. S. Jameel, and M. A. Dheyab, "Mycosynthesis of gold nanoparticles using the extract of Flammulina velutipes, Physalacriaceae, and their efficacy for decolorization of methylene blue," *J. Environ. Chem. Eng.*, vol. 8, no. 3, p. 103841, 2020, doi: 10.1016/j.jece.2020.103841.

[90] J. Das and P. Velusamy, "Catalytic reduction of methylene blue using biogenic gold nanoparticles from Sesbania grandiflora L," *J. Taiwan Inst. Chem. Eng.*, vol. 45, no. 5, pp. 2280–2285, 2014, doi: 10.1016/j.jtice.2014.04.005.

[91] V. S. Suvith and D. Philip, "Catalytic degradation of methylene blue using biosynthesized gold and silver nanoparticles," *Spectrochim. Acta - Part A Mol. Biomol. Spectrosc.*, vol. 118, pp. 526–532, 2014, doi: 10.1016/j.saa.2013.09.016.